

## RESEARCH ARTICLE

# Regulation of macrophage IFN $\gamma$ -stimulated gene expression by the transcriptional coregulator CITED1

Aarthi Subramani<sup>1</sup>, Maria E. L. Hite<sup>1</sup>, Sarah Garcia<sup>1</sup>, Jack Maxwell<sup>1</sup>, Hursha Kondes<sup>1</sup>, Grace E. Millican<sup>1</sup>, Erin E. McClelland<sup>2</sup>, Rebecca L. Seipelt-Thiemann<sup>1</sup> and David E. Nelson<sup>1,\*</sup>

## ABSTRACT

Macrophages serve as a first line of defense against microbial pathogens. Exposure to interferon- $\gamma$  (IFN $\gamma$ ) increases interferon-stimulated gene (ISG) expression in these cells, resulting in enhanced antimicrobial and proinflammatory activity. Although this response must be sufficiently vigorous to ensure the successful clearance of pathogens, it must also be carefully regulated to prevent tissue damage. This is controlled in part by CBP/p300-interacting transactivator with glutamic acid/aspartic acid-rich carboxyl-terminal domain 2 (CITED2), a transcriptional coregulator that limits ISG expression by inhibiting STAT1 and IRF1. Here, we show that the closely related *Cited1* is an ISG, which is expressed in a STAT1-dependent manner, and that IFN $\gamma$  stimulates the nuclear accumulation of CITED1 protein. In contrast to CITED2, ectopic CITED1 enhanced the expression of a subset of ISGs, including *Ccl2*, *Ifit3b*, *Isg15* and *Oas2*. This effect was reversed in a *Cited1*-null cell line produced by CRISPR-based genomic editing. Collectively, these data show that CITED1 maintains proinflammatory gene expression during periods of prolonged IFN $\gamma$  exposure and suggest that there is an antagonistic relationship between CITED proteins in the regulation of macrophage inflammatory function.

This article has an associated First Person interview with the first author of the paper.

**KEY WORDS:** Macrophage, Macrophage polarization, Interferon- $\gamma$ , CITED1, STAT1

## INTRODUCTION

Macrophages are multifunctional innate immune cells that play a major role in the maintenance of tissue homeostasis (Ginhoux and Jung, 2014). These tissue-associated phagocytic cells respond rapidly to injury and infection, initiating an appropriate inflammatory response and clearing microbial pathogens and cellular debris before participating in wound-healing and attenuating inflammatory signals as the infection is resolved. As part of this process, macrophages detect and respond to microbial ligands using pattern recognition receptors (PRRs), including the toll-like receptor family (TLRs) of proteins. These stimulate the activity of nuclear factor  $\kappa$ -light-chain-enhancer of activated B cells (NF- $\kappa$ B) and other proinflammatory transcriptional

regulators, that increase the expression of cytokines, chemokines and anti-microbial proteins, such as inducible nitric oxide synthase (iNOS) (Dorrington and Fraser, 2019; Fitzgerald and Kagan, 2020; Kim et al., 1997). This response is modified or enhanced by a variety of endogenous factors, including interferon- $\gamma$  (IFN $\gamma$ ), which is largely produced by T cells and natural killer cells (Gill et al., 2011).

IFN $\gamma$ , also known as type II interferon, is a pleiotropic cytokine capable of regulating the activity of innate and adaptive immunity, and is associated with the response to viral and non-viral pathogens (Schroder et al., 2004). Within the context of innate immunity, IFN $\gamma$  stimulates classical activation or M1 polarization of macrophages (Murray et al., 2014), a heightened proinflammatory anti-microbial state that is important for the successful clearance of bacterial and eukaryotic pathogens, including the fungal pathogen *Cryptococcus neoformans* (Hardison et al., 2012; Hardison et al., 2010; Leopold Wager et al., 2014, 2015). This transition to the M1 state is accompanied by extensive transcriptional reprogramming, involving over 1000 genes (Beyer et al., 2012; Jablonski et al., 2015). These changes in gene expression are largely directed by the transcription factors signal transducer and activator of transcription 1 (STAT1) and interferon regulated factor 1 (IRF1), operating individually or in concert at IFN $\gamma$ -stimulated gene (ISG) promoters (Michalska et al., 2018).

IFN $\gamma$  homodimers stimulate STAT1 activity by binding to and facilitating the assembly of tetrameric interferon- $\gamma$  receptor (IFNGR) complexes from dimers of IFNGR1 and IFNGR2. This activates receptor-associated Janus kinase (JAK) 1 and 2 by transphosphorylation within the cell, which subsequently tyrosine-phosphorylate the cytosolic domain of IFNGR1. This enables STAT1 proteins to dock with the receptor complex via phospho-tyrosine-binding Src-homology-2 (SH2) domains, bringing these transcription factors into proximity with the activated JAK proteins, which phosphorylate Y701 within the STAT1 C-terminus. The same SH2 domains used for receptor binding also facilitate the homodimerization of phosphorylated STAT1 proteins, creating  $\gamma$ -activated factors (GAFs). These GAFs translocate to the nucleus and initiate a first phase of ISG expression through binding to STAT1 target promoters that contain palindromic  $\gamma$ -activated sites (GAS) (Decker et al., 1997). This includes the *Irf1* gene, and newly synthesized IRF1 proteins then participate in the regulation of a second wave of gene expression through binding interferon-stimulated response elements (ISREs) and IRF-response elements in ISG promoters (Kroger et al., 2002; Pine et al., 1990). These include interferon-induced protein with tetratricopeptide repeat 1 (*Ifit1*), interferon-stimulated gene 15 (*Isg15*), MX dynamin like GTPase 1 (*Mx1*) and 2'-5'-oligoadenylate synthase 1 (*Oas1*) (Michalska et al., 2018). Additionally, IRF1 and STAT1 co-regulate genes that contain both GAS and ISRE cis-regulatory sites (Chatterjee-Kishore et al., 1998; Kumatori et al., 2002; Ramsauer et al., 2007). This includes *Irf9*, bone marrow stromal cell antigen 2 (*Bst2*) and interferon induced transmembrane protein 1

<sup>1</sup>Department of Biology, Middle Tennessee State University, Murfreesboro, TN 37132, USA. <sup>2</sup>College of Osteopathic Medicine, Marian University, Indianapolis, IN 46222, USA.

\*Author for correspondence (david.e.nelson@mtsu.edu)

© A.S., 0000-0003-1094-9554; R.L.S.-T., 0000-0001-5265-7897; D.E.N., 0000-0002-5034-0885

Handling Editor: Daniel Billadeau

Received 17 August 2022; Accepted 21 November 2022

(*Ifitm1*) (Ogony et al., 2016; Ohtomo et al., 1999; Testoni et al., 2011), but also *Stat1* itself, constituting a positive-feedback loop (Wong et al., 2002).

To prevent tissue damage that accompanies uncontrolled or prolonged inflammation, macrophage IFN $\gamma$  signaling is restrained by a variety of mechanisms (Murray and Smale, 2012; Shuai and Liu, 2003; Wang et al., 2014). It is antagonized by the anti-inflammatory cytokines interleukin-4 (IL-4) and IL-13, which promote an alternative activation or M2 polarization state, and the downregulation of many ISGs. Negative feedback also occurs through expression of cell-intrinsic factors, including suppressor of cytokine signaling 1 (Socs1), an ISG co-regulated by STAT1 and IRF1 that functions as a potent inhibitor of IFN $\gamma$  signaling at the JAK level (Alexander et al., 1999; Liau et al., 2018; Wilson, 2014; Yoshimura et al., 2007). More recently, CBP/p300-interacting transactivator with glutamic acid (E) and aspartic acid (D)-rich tail 2 (CITED2) has been identified as a transcriptional co-regulator that operates at the chromatin and/or promoter level to attenuate macrophage proinflammatory gene expression (Kim et al., 2018).

CITED2 is one of three CITED family proteins present in mammalian systems (CITED1, CITED2 and CITED4; Andrews et al., 2000; Braganca et al., 2002; Shioda et al., 1996; Yahata et al., 2002). As they are unable to bind directly to DNA, CITED proteins increase or inhibit the expression of genes by facilitating or preventing transcription factors from forming chromatin complexes with the histone acetyltransferase, CREB-binding protein (CBP; also known as CREBBP) or its paralog p300 (also known as EP300) (collectively denoted CBP/p300). These interactions require a C-terminal conserved region 2 (CR2) domain common to all CITED family proteins (Yahata et al., 2000) and an unstructured N-terminal region that differs between CITED proteins. Although the CR2 domains bind cysteine-histidine (CH; also known as TAZ) domains within CBP/p300, the unique N-terminus of each CITED family protein facilitates interactions with different sets of transcription factors. In this way, CITED proteins operate as adaptors, stabilizing transcription factor–CBP/p300 complexes. However, they can also block the formation of other complexes competitively in instances where transcription factors interact with CBP/p300 via the same CH domain as the CITED protein. For example, CITED2 is constitutively expressed in myeloid cells, including macrophages, and localizes exclusively to the nucleus in complex with CBP/p300 (Bhattacharya et al., 1999). Here, it restricts the ability of hypoxia-inducible factor 1  $\alpha$  (HIF1 $\alpha$ ) and p65 (RelA)-containing NF- $\kappa$ B transcription factors to access the CH1 domain of CBP/p300, thereby reducing proinflammatory gene expression (Bhattacharya et al., 1999; Freedman et al., 2003; Leung et al., 1999; Lou et al., 2011; Pong Ng et al., 2020). In fact, synthetic constrained peptides derived from the CR2 domain of CITED2 function as potent inhibitors of HIF1 $\alpha$  signaling (Qin et al., 2021). CITED2 has also been shown to repress both STAT1- and IRF1-dependent ISGs in bone-marrow-derived macrophages and RAW264.7 macrophage-like cells, likely by a similar mechanism (Zafar et al., 2021).

Until recently, CITED2 was thought to be the only CITED family member expressed in macrophages (Kim et al., 2018). In this study, we show that IFN $\gamma$  stimulation promotes expression of *Cited1* in a STAT1-dependent manner and nuclear accumulation of CITED1 proteins. Unlike CITED2, expression of ectopic CITED1 largely enhanced the expression of STAT1- and IRF1-dependent ISGs in IFN $\gamma$ -stimulated macrophages, and this was reversed in *Cited1*-null cells. As CITED1 expression is featured as part of a later wave of ISGs, these data indicate that it might serve as a mechanism to

prolong the IFN $\gamma$  response for a subset of STAT1- and IRF1-regulated genes.

## RESULTS

### CITED1 and CITED2 respond differently to M1 polarizing stimuli

Over the past few years, *Cited2* has been found to play an important role in innate immune function (Aguirre and Gibson, 2000; Kim et al., 2018; Lou et al., 2011; Pong Ng et al., 2020; Zafar et al., 2021). CITED2 is highly expressed at both the transcript and protein level in monocytes and macrophages of murine and human origin (Kim et al., 2018), it is vital for the development of these cells (Chen et al., 2007; Kranc et al., 2009), and attenuates proinflammatory gene expression by acting as an inhibitor of NF- $\kappa$ B, HIF1 $\alpha$ , STAT1 and IRF1 transcriptional regulators (Kim et al., 2018; Pong Ng et al., 2020; Zafar et al., 2021). In contrast, expression of the two other mammalian *Cited* family members, *Cited1* and *Cited4*, have been documented as either undetectable or expressed at ~100-fold lower levels than *Cited2*, which suggest they have no biological role in macrophages (Kim et al., 2018). However, in our previous study, we showed that infection of M1 polarized RAW264.7 murine macrophages with *C. neoformans* promotes transcriptional upregulation of *Cited1* (Subramani et al., 2020). A more detailed reanalysis of these data comparing vehicle- and IFN $\gamma$ -treated cells showed that IFN $\gamma$  stimulation alone was sufficient to induce *Cited1* (Fig. 1A), raising the possibility that *Cited1* expression is a feature of M1 polarization and *Cited1* might also be an ISG.

To validate this result and investigate the dynamics of IFN $\gamma$ -stimulated *Cited1* expression, RNA was harvested from RAW264.7 cells at 3, 6, 12, 24 and 48 h post-IFN $\gamma$  treatment, and *Cited1* transcript levels were measured using qRT-PCR. Here, *Cited1* expression was apparent at 24 h, and was further increased by 48 h post-stimulation (>300-fold increase in  $t=0$  versus 48 h; Fig. 1B), and this was mirrored at the protein level (Fig. 1C). This differs from the reported effects of M1 polarizing stimuli on *Cited2* expression, which has been shown to be repressed by IFN $\gamma$  or lipopolysaccharide (LPS) at 6 h post-treatment (Kim et al., 2018). We also observed a similar decrease in *Cited2* transcript levels post-IFN $\gamma$  treatment, but this was transient and not statistically significant, with *Cited2* returning to basal levels within 24 h (Fig. 1D). To explore the effects of other M1 polarizing stimuli on *Cited1* and *Cited2* expression, macrophages were treated with LPS alone and in combination with IFN $\gamma$ . Here, LPS had no effect on *Cited1* expression and did not enhance IFN $\gamma$ -stimulated expression of the gene (Fig. 1E). In contrast, LPS or IFN $\gamma$  treatment alone had no effect on *Cited2* expression at 24 h post-stimulus (Fig. 1F). However, IFN $\gamma$  and LPS co-treatment stimulated a >4-fold increase in *Cited2* expression compared to vehicle. These contrasting expression patterns indicate that *Cited1* and *Cited2* are regulated differently and likely play distinct roles in modulating the macrophage transcriptome, as each operates on a differing timescale and in a stimulus-dependent fashion.

To further explore the notion that regulation of *Cited1* and *Cited2* differ, the expression of *Cited* family genes was examined using the open access Genotype-Tissue Expression (GTEx) database, which contains searchable gene expression data based on the molecular analysis of 54 non-diseased human tissue sites from ~1000 individuals (GTEx Consortium, 2013). This showed that the expression of *Cited1* and *Cited2* was strikingly different. Whereas *Cited2* expression was near ubiquitous, being expressed in most tissues, *Cited1* expression was largely restricted to the testis and

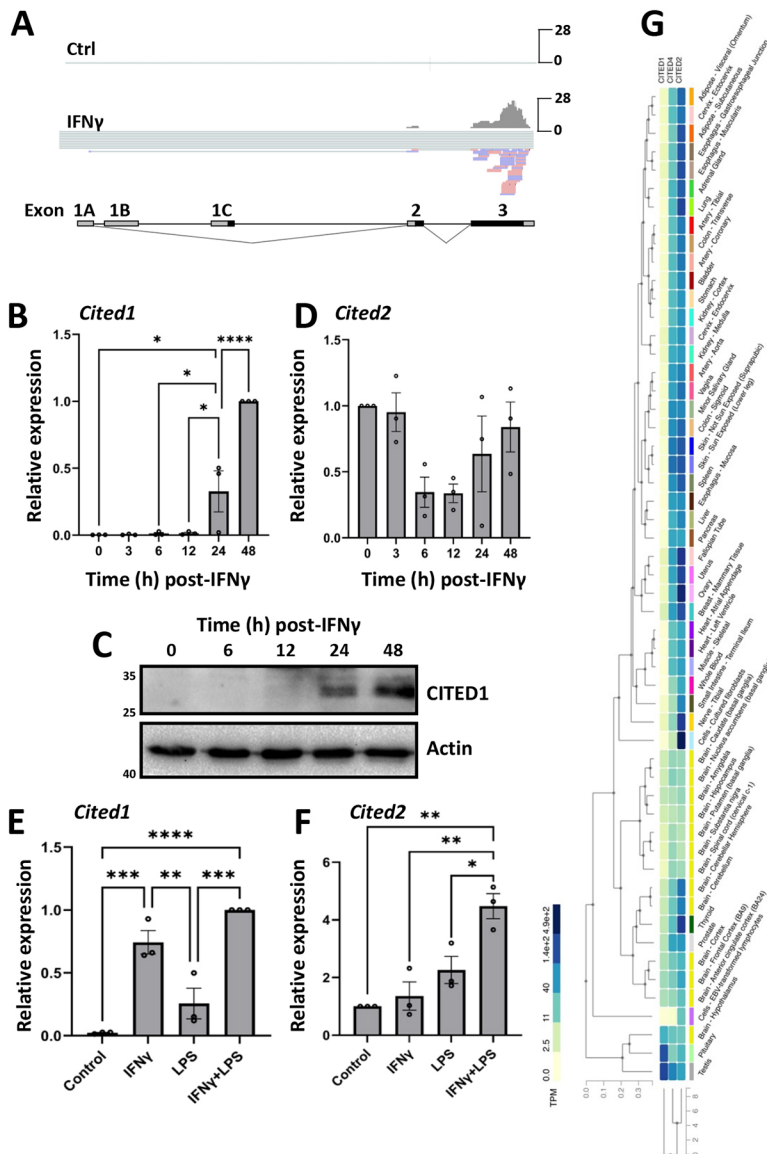


**Fig. 1. *Cited1* is an IFN $\gamma$ -responsive gene.** (A) RNA-seq analysis was performed on mRNA extracted from RAW264.7 cells treated with or without IFN $\gamma$  for 24 h. Reads were aligned to the *Cited1* gene using Integrated Genome Viewer. Protein coding regions of exons are marked in black. An individual representative repeat (1 of 3) is shown for each condition. (B–F) RAW264.7 cells were incubated with IFN $\gamma$  for the indicated times (B–D) or IFN $\gamma$  and/or LPS (E,F) for 24 h then RNA and proteins were harvested. (B,D–F) Expression of *Cited1* and *Cited2* transcripts were measured by qRT-PCR. Error is represented as s.e.m. ( $n=3$ ). \* $P<0.05$ ; \*\* $P<0.01$ ; \*\*\* $P<0.001$ ; \*\*\*\* $P<0.0001$  (one-way ANOVA followed by a Tukey's multiple comparison test). (C) CITED1 protein levels were measured by western blotting; a representative experiment out of three repeats is shown. (G) GTEx analysis of *Cited* family member expression across 54 different non-diseased tissues.

pituitary gland (Fig. 1G). These differences are corroborated by experimental data showing that although both *Cited1* and *Cited2* are expressed in the developing kidney, only *Cited2* persists in mature renal structures (Boyle et al., 2007). Collectively, these data indicate that *Cited1* and *Cited2* are regulated differently and are unlikely to be functionally redundant in macrophages and other contexts.

### Regulation of *Cited1* expression by STAT1

Although differences in transcriptional regulation of the murine *Cited1* and *Cited2* gene are now clear, the finer detail of *Cited1* gene expression is lacking. Prior studies have shown that the 1.0 kb region immediately upstream of the TATA box has promoter activity and contains putative binding sites for Sp1, Oct-1 (also known as POU2F1) and AP-2, although none of these have been experimentally confirmed (Fenner et al., 1998). From these data, it is unclear how IFN $\gamma$  stimulates *Cited1* expression in macrophages.

Although engagement of IFN $\gamma$  receptors activates a range of signaling pathways (Ramana et al., 2002), the JAK-STAT pathway is considered the central coordinator of the transcriptional response, with STAT1 transactivating ISGs directly or via IRF1 (Durbin et al.,

1996; Meraz et al., 1996), which is itself a STAT1-regulated gene (Decker et al., 1997; Sikorski et al., 2012) (Fig. 2A). To investigate whether *Cited1* is regulated by the STAT1-IRF1 axis, we scanned a region spanning  $-2000$  to  $100$  bp relative to the transcriptional start site of the murine *Cited1* gene using the Eukaryotic Promoter Database (Swiss Institute of Bioinformatics) for transcription factor binding sites (Dreos et al., 2017, 2015). A total of three STAT1 (at  $-18$ ,  $-724$  and  $-1038$ ) and two IRF1 (at  $-1237$  and  $-1297$ ) putative cis-regulatory sites were identified (cut-off at  $P<0.001$ ; Fig. 2B). Based on these data, we hypothesized that IFN $\gamma$ -stimulated *Cited1* expression is regulated by the STAT1-IRF1 axis.

To test this, RAW264.7 cells were transduced with a lentiviral construct to express the Cas9 endonuclease and either a non-targeting 'scramble' guide RNA (gRNA) or a gRNA targeting exon 9 of the *Stat1* gene. As *Irf1* expression is STAT1 dependent, this manipulation was designed to ablate the activity of both transcription factors in these cells. In cells expressing the STAT1-targeting gRNA, the loss of basal STAT1 protein expression was confirmed by western blotting (Fig. 2C). To further validate these cells, the expression of *Isg20* and *Ifit1*, known transcriptional targets



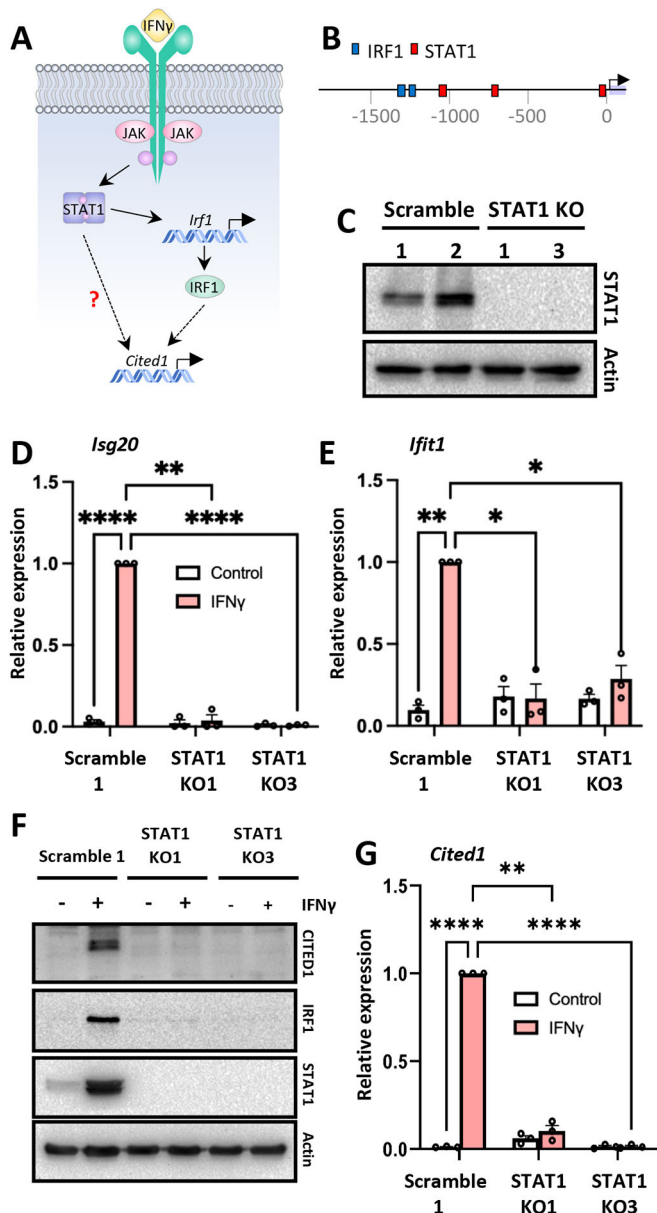


**Fig. 2. Expression of *Cited1* is STAT1-dependent.** (A) Diagram of the IFN $\gamma$ -STAT1 signaling pathway. The relationship under investigation is demarcated by a question mark. (B) Putative STAT1 and IRF1 transcription factor binding sites were detected in the murine *Cited1* promoter using EPD and a  $P$ -value cutoff of  $\leq 0.001$ . (C) Western blot analysis for STAT1 proteins in two independent clonal RAW264.7 cell lines stably transduced with lentiviral constructs to express Cas9 and either non-targeting (scramble) or *Stat1*-targeting gRNA. (D–G) RAW264.7 STAT1 knockout (KO) cells and scramble controls were stimulated with IFN $\gamma$  for 48 h. Expression of (D) *Isg20* and (E) *Ifit1* was measured by qRT-PCR. (F) STAT1, IRF1 and CITED1 proteins were detected by western blotting, and (G) *Cited1* expression was measured by qRT-PCR. Error is represented as s.e.m. ( $n=3$ ). A representative experiment out of three repeats is shown for C and F. \* $P<0.05$ ; \*\* $P<0.01$ ; \*\*\*\* $P<0.0001$  (one-way ANOVA followed by a Tukey's multiple comparison test).

of the STAT1-IRF1 axis (Gongora et al., 2000), were measured by qRT-PCR. Here, we found that IFN $\gamma$ -stimulated expression of these genes was lost in the STAT1-null cells (Fig. 2D,E). Finally, it was also confirmed that IFN $\gamma$ -stimulated IRF1 protein expression was ablated in the STAT1-null cells by western blot analysis (Fig. 2F).

As predicted, IFN $\gamma$ -stimulated CITED1 protein expression was detected in the scramble control cells but not STAT1-null cells (Fig. 2F). This result was confirmed at the RNA level, where *Cited1* RNA expression was abrogated in both STAT1-null clonal lines but remained robust in the scramble controls ( $\sim 80$ -fold increase in IFN $\gamma$  stimulated cells; Fig. 2G). The increased STAT1 protein expression observed in the control cells is consistent with the known effects of IFN $\gamma$  priming on STAT1 expression (Fig. 2F) (Hu et al., 2002, 2005). Collectively, these data indicate that the *Cited1* gene is downstream of the JAK-STAT portion of the pathway and requires the STAT1 transcription factor, although it is unclear whether STAT1 directly regulates *Cited1* or whether *Cited1* resides further down the pathway.

### IFN $\gamma$ -stimulated nuclear translocation of CITED1

To function as a transcriptional co-regulator, CITED1 must be present in the nucleus. However, its subcellular localization varies among cell types and is cytosolic in most cells, likely due to a nuclear export sequence present within the CR2 domain (Howlin et al., 2006; Shi et al., 2006). To determine the localization of the protein in macrophages, RAW264.7 cells were stably transduced with pINDUCER20-EYFP-CITED1 to express full-length murine CITED1 with an N-terminal enhanced yellow fluorescent protein (EYFP) tag under the control of a doxycycline (dox)-dependent promoter. Cells were incubated with dox to induce EYFP-CITED1 prior to cytokine stimulation. Prior to IFN $\gamma$  treatment, EYFP-CITED1 was predominantly cytosolic in all cells (Fig. 3A,B). However, IFN $\gamma$  stimulated the relocalization of the protein, with EYFP-CITED1 becoming enriched in the nucleus by 24 h post-stimulation and remaining there for at least a further 24 h post-treatment (Fig. 3A,B).

Phosphorylation has also been shown to affect CITED1 localization. In MC3T3-E1 murine osteoblasts, parathyroid hormone (PTH) stimulates the expression and nuclear translocation of CITED1 proteins as part of the osteoblastic differentiation process (Lin et al., 2014; Yang et al., 2008). Here, the nuclear accumulation of CITED1 required the protein kinase C (PKC)-dependent phosphorylation of the protein at S79 (Lin et al., 2014). To test whether phosphorylation of CITED1 accompanied IFN $\gamma$ -induced nuclear translocation, we generated RAW264.7 cells that expressed untagged CITED1 protein in a dox-dependent manner (DI-CITED1). This decoupled CITED1 expression from IFN $\gamma$  stimulation and allowed cells to produce a preexisting pool of exogenous CITED1. The phosphorylation state of these proteins was measured pre- and post-IFN $\gamma$  treatment. Although there are currently no antibodies available to directly detect phosphorylated forms of the protein, phosphorylation has been shown to reduce the mobility of CITED1 on SDS-PAGE gels (Shi et al., 2006). Prior to IFN $\gamma$  treatment, CITED1 appeared as two major bands, a high mobility band and a fainter low mobility band (Fig. 3C). However, in cells incubated with IFN $\gamma$  for 24 h, only the low-mobility CITED1 band was apparent, suggesting that the cellular pool of CITED1 proteins transition from a largely dephosphorylated state to a mostly phosphorylated state upon treatment with IFN $\gamma$ . The appearance of the higher molecular mass band was eliminated by  $\lambda$  protein phosphatase ( $\lambda$ PP) treatment of the samples prior to western blotting, confirming that this band was associated with phosphorylated forms of CITED1 and was not caused by other post-translational modifications (Fig. 3D). Collectively, these data raise the possibility that IFN $\gamma$  regulates the localization of CITED1 in a phosphorylation-dependent manner, similar to PTH-stimulated nuclear translocation of CITED1 in osteoblasts.

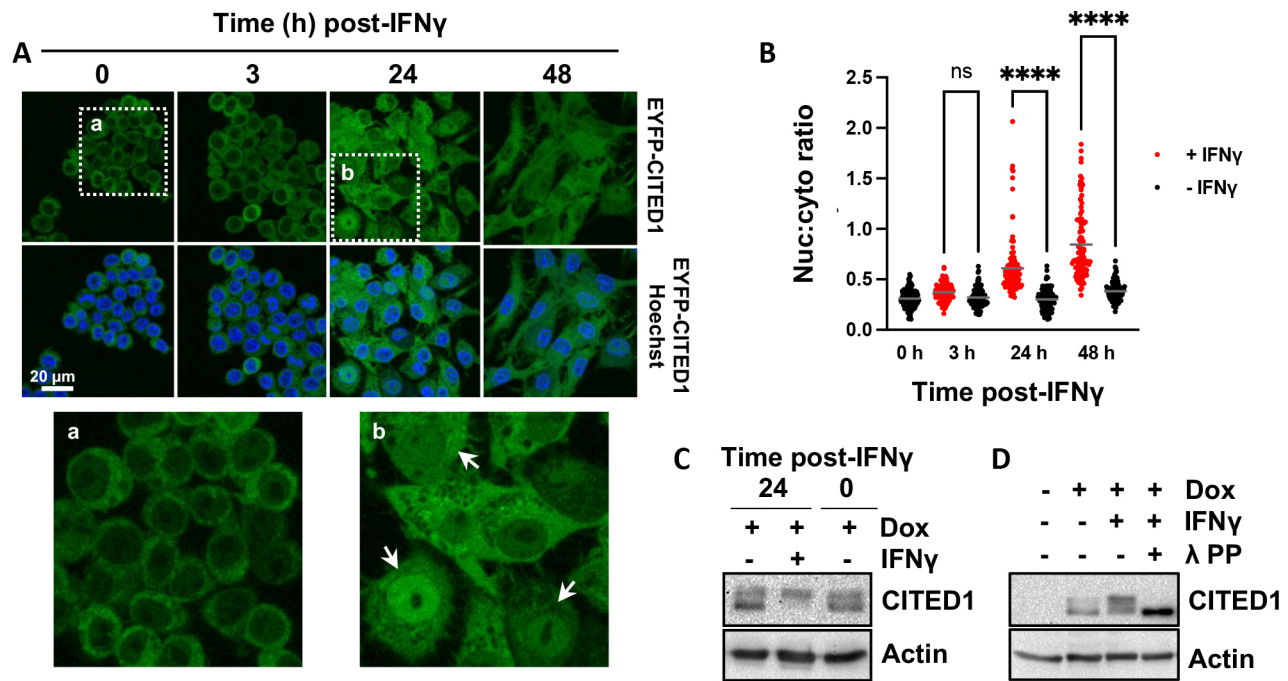


**Fig. 3. IFN $\gamma$  stimulates nuclear translocation and phosphorylation of CITED1.** (A) RAW264.7 stably transduced with lentiviral constructs to express EYFP-CITED1 from a dox-inducible promoter (DI-EYFP-CITED1 cells). Cells were incubated with dox for 24 h prior to co-treatment with IFN $\gamma$  for the indicated times and visualized by live cell confocal microscopy. Arrows mark cells where the nuclear to cytoplasmic ratio (nuc:cyto) for EYFP-CITED1 is  $\geq 1$ . (B) Quantification of nuc:cyto EYFP-CITED1 in individual cells from the experiment described in A. Data are plotted for  $\geq 100$  cells/condition and the mean is marked. \*\*\*\* $P < 0.0001$ ; ns, not significant (one-way ANOVA followed by a Tukey's multiple comparison test). (C) DI-CITED1 cells were incubated with dox for 24 h to stimulate CITED1 expression prior to co-treatment with IFN $\gamma$  or vehicle for a further 24 h. Low- and high-mobility CITED1 species were detected by western blotting. (D) DI-CITED1 cells were treated as described in C but lysed at 6 h post-IFN $\gamma$  in a non-denaturing 1% triton X-100 buffer. Lysates were incubated with or without  $\lambda$ PP for 30 min prior to western blot analysis for CITED1. A representative experiment out of three repeats is shown for C and D.

### CITED1 enhances the expression of a subset of ISGs

As IFN $\gamma$  treatment promoted nuclear accumulation of CITED1, we speculated that it might also function as a transcriptional co-regulator under these conditions. CITED2, which is constitutively nuclear, inhibits proinflammatory gene expression by competing with NF- $\kappa$ B and HIF-1 transcription factors for binding of the CH1 domain of CBP/p300 (Bhattacharya et al., 1999; Lou et al., 2011). Additionally, and of particular relevance to this study, overexpression of CITED2 in RAW264.7 macrophages inhibits IFN $\gamma$ -stimulated expression of genes regulated by the STAT1-IRF1 axis, including *Irf1*, *Irg1* (also known as *Acod1*), *F3*, *Tmem140* and *Dnase113* (Zafar et al., 2021). Although CITED1 is also known to interact with CBP/p300, the two CITED family proteins exhibit differing binding preferences for the CH domains in CBP/p300; CITED1 only weakly interacts with the CH1 domain and instead shows a preference for the central CH2 domain (Yahata et al., 2000), distant from known STAT1-binding regions (Zhang et al., 1996). For this reason, we hypothesized that CITED1 might have distinct effects on STAT1- and IRF1-dependent gene expression. To explore this, the DI-CITED1 cell line was utilized as part of a gain-of-function strategy, measuring the effect of ectopic CITED1 expression on IFN $\gamma$ -stimulated gene expression. In brief, gene expression changes were measured 24 h post-IFN $\gamma$  by RNAseq-based transcriptome profiling with and without prior dox incubation (Fig. 4A). Corresponding control samples were prepared using unmodified RAW264.7 cells to identify and exclude gene expression changes stimulated by dox alone.

An initial assessment of the transcriptome data performed using a CuffDiff-based analysis pipeline identified 724 differentially expressed genes (DEGs) in a pairwise comparison of

IFN $\gamma$ -stimulated cells with and without dox treatment (IFN $\gamma$  versus dox+IFN $\gamma$ ; Table S1). These data showed increased expression of multiple members of gene families closely associated with the response to IFN $\gamma$  in CITED1 over-expressing cells, including members of the C-C motif chemokine ligand (*Ccl1*, *Ccl2*, *Ccl3*, *Ccl4* and *Ccl7*), *Ifit1* (*Ifit1*, *Ifit3* and *Ifit3b*) and *Isg* (*Isg15* and *Isg20*) gene families. A selection of these were validated by qRT-PCR together with *Cd40* and *Cd52*, which encode surface markers that were also upregulated upon CITED1 overexpression (Fig. 4B). Notably, increased expression of multiple genes that were upregulated in CITED2-knockout bone marrow-derived macrophages (BMDMs) were observed, including *Mxd1*, *Il17ra*, *Tmem140*, *Cd86* and *Scimp* (Zafar et al., 2021), supporting the notion that CITED1 and CITED2 had opposing effects on IFN $\gamma$ -stimulated gene expression.

Top biological process (BP) gene ontology (GO) terms associated with DEGs from the IFN $\gamma$  versus dox+IFN $\gamma$  pairwise comparison included 'Defense response to virus', 'Innate immune response' and 'Inflammatory response', which is indicative that CITED1 expression affected the expression of gene sets fundamental to the IFN $\gamma$  response (Fig. 4C). Protein interaction network analysis was performed in STRING, which also allowed for the visualization of changes in the IFN $\gamma$  response stimulated by CITED1 expression (Fig. 4D). Here, genes clusters associated with cytokines and chemokines [GO term 'Regulation of cytokine production'; false discovery rate (FDR)  $2.57 \times 10^{-9}$ ], apoptosis (GO term 'Regulation of apoptotic process'; FDR  $3.9 \times 10^{-4}$ ) and a smaller cluster of genes associated with the complement system were observed.

To more formally assess the impact of CITED1 expression on the transcriptional changes that accompany IFN $\gamma$ -stimulated M1

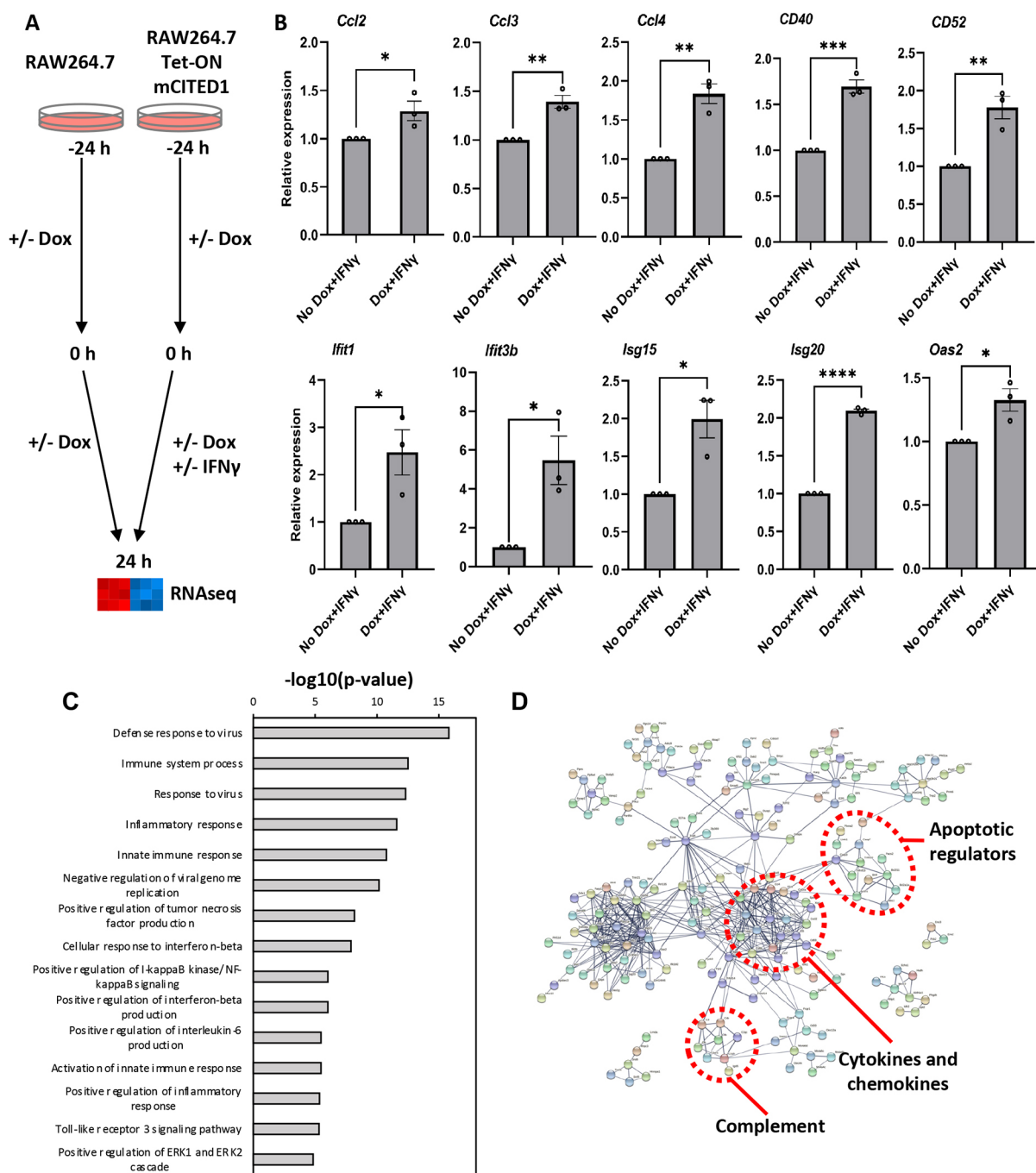


**Fig. 4. CITED1 enhances IFN $\gamma$ -stimulated gene expression.** (A) Design of CITED1 overexpression transcriptome profiling experiment. RAW264.7 DI-CITED1 cells were incubated with or without dox for 24 h to overexpress CITED1 prior to co-treatment with IFN $\gamma$  or vehicle for a further 24 h. Following treatments, total RNA was harvested for RNAseq. (B) Select CITED1-regulated genes identified by the RNAseq screen were validated by qRT-PCR. Results are mean $\pm$ s.e.m. ( $n=3$ ). (C) GO analysis was performed in DAVID on DEGs from a pairwise comparison of DI-CITED1 cells treated as indicated (no dox+IFN $\gamma$  versus with dox+IFN $\gamma$ ). Top biological process (BP) GO terms are ranked by  $-\log(P\text{-value})$ . (D) STRING analysis was performed on the same set of DEGs. Boundaries enclosing gene clusters denote gene sets with a common function, as identified using the KEGG analysis tools in STRING.

polarization, the IFN $\gamma$  versus dox+IFN $\gamma$  DEG set was compared to corresponding DEGs from a comparison of untreated control and IFN $\gamma$ -treated cells (Ctrl versus IFN $\gamma$ ). Of the 2775 DEGs between control and IFN $\gamma$ -stimulated cells, 300 (10.8%) were affected by CITED1 overexpression (Fig. 5A), which corresponded to 41.5% of all DEGs from the IFN $\gamma$  versus dox+IFN $\gamma$  pairwise comparison. Of those genes common to both pairwise comparisons, the majority (255; 85%) were concordant (Fig. 5B), indicating that

CITED1 expression enhanced the effect of IFN $\gamma$  stimulation on a subset of IFN $\gamma$ -responsive genes. These shared concordant genes included *Isg15*, *Isg20*, various *Ifit* family genes, and the cytokines *Ccl2* and *Ccl4* (Table S2). GO analysis of this shared pool of DEGs revealed an enrichment in genes associated with macrophage antiviral function (Fig. 5C), as indicated by the GO terms ‘Defense response to virus’ ( $P=6.84\times 10^{-17}$ ; FDR=1.24 $\times 10^{-13}$ ) and ‘Negative regulation of



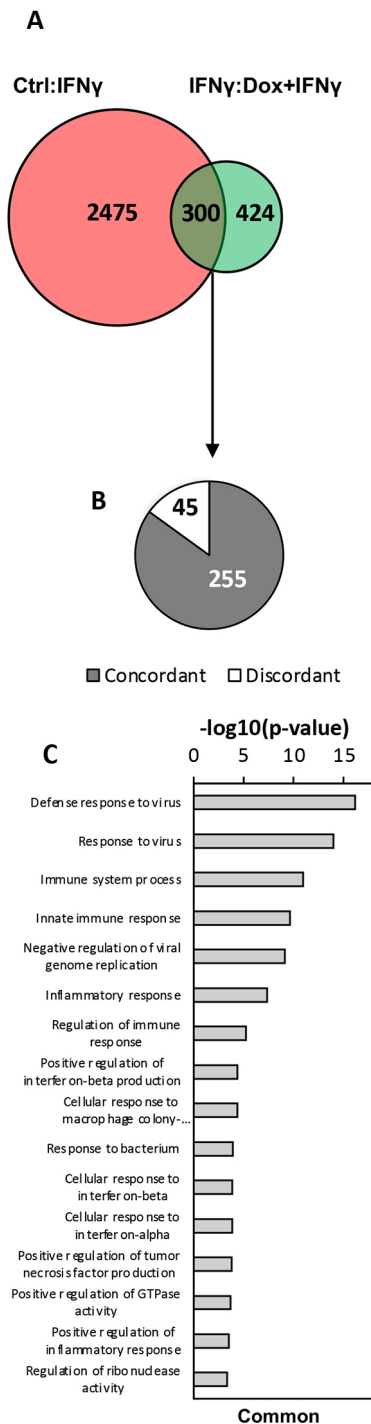


**Fig. 5. Effect of CITED1 expression on the M1 transcriptome.** (A) Venn diagram to represent shared and DEGs between pairwise comparisons of DI-CITED1 cells treated as follows: no dox and no IFN $\gamma$  (control) versus no dox with IFN $\gamma$  (Ctrl:IFN $\gamma$ ), and with IFN $\gamma$  and no dox versus with dox with IFN $\gamma$  (IFN $\gamma$ :dox+IFN $\gamma$ ). (B) Of the 300 DEGs common to Ctrl:IFN $\gamma$  and IFN $\gamma$ :dox+IFN $\gamma$ , 255 (85%) were regulated in the same way (up versus down) (concordant; grey) and 45 (15%) were discordant. (C) GO analysis was performed in DAVID on common DEGs from the comparison shown in A. Top biological process (BP) GO terms are ranked by  $-\log(P\text{-value})$ .

viral genome replication ( $P=7.49\times 10^{-10}$ ;  $FDR=2.72\times 10^{-7}$ ). Overall, these data show that CITED1 expression potentiates the effects of IFN $\gamma$  stimulation on select ISGs.

### CITED1 modulates the expression of STAT1 and IRF1 target genes

As an alternative method to examine the effect of CITED1 on ISG expression, the IFN $\gamma$  versus dox+IFN $\gamma$  dataset was reanalyzed using gene set enrichment analysis (GSEA), a statistical tool used to identify phenotypic differences between transcriptome datasets for specific functional gene sets (Subramanian et al., 2005). In addition to identifying the top up- and down-regulated genes (Fig. 6A), the 'Interferon gamma response' gene set was identified as significant among the hallmark gene sets. This produced a negative normalized enrichment score (NES;  $-1.56$ ), suggestive of an enhanced IFN $\gamma$  response in CITED1 overexpressing cells (Fig. 6B,C).

As the CuffDiff and GSEA analysis identified genes containing ISRE cis-regulatory sites, such as *Ifit3*, *Mx1* and *Isg15* (Bluyssen et al., 1994; Ronni et al., 1998; Testoni et al., 2011), as well as genes containing both or composite ISREs and GAS, including *Bst2* (Ohtomo et al., 1999; Wong et al., 2002; Yan et al., 1995), it was plausible that CITED1 affected both STAT1- and IRF1-dependent signaling. This was tested computationally in GSEA using custom STAT1- and IRF1-regulated genes lists. Genes included in these lists [provided by the Mahbeleswar laboratory, Case Western University (Zafar et al., 2021)] were identified based on gene expression changes observed in STAT1- and IRF1-knockout macrophages following IFN $\gamma$  treatment (Langlais et al., 2016; Semper et al., 2014). This analysis indicated that CITED1 overexpression disproportionately enhanced the expression of genes identified as regulated by STAT1 (Fig. 6D,E) and IRF1 (Fig. 6F,G). This is consistent with the notion that CITED1 and CITED2 have opposing effects on ISG expression as CITED2-null BMDMs show increased expression of STAT1 and IRF1 target genes (Zafar et al., 2021).

### CITED1 knockout attenuated the transcription response to IFN $\gamma$

As our gain-of-function experiments indicated that CITED1 functions as a positive regulator of select ISGs, corresponding loss-of-function experiments were performed to verify this result. For these, a RAW264.7 cell line with a null *Cited1* allele was produced using CRISPR/Cas9 and gRNA targeting exon 3 of the gene (Fig. 7A). As RAW264.7 cells are derived from male BALB/c mice, they contain a single copy of the X-chromosome-encoded *Cited1* gene. Therefore, INDELs produced by CRISPR gene-editing were hemizygous. These were characterized by sequencing a 1.5 kb region surround the sgRNA-binding site (Fig. 7B). Of the 17 clones screened, nine contained frameshifts resulting in premature stop codons. Clones 6 and 9 both showed a loss of *Cited1* mRNA and protein expression, as measured by multiplex RT-PCR and western blotting, respectively (Fig. 7C,D).

To appraise the effect of CITED1 loss on ISG expression, the transcriptome of CITED1-null cells (clone 9) was compared to RAW264.7 cells stably expressing Cas9 and a non-targeting scramble gRNA at 48 h post-IFN $\gamma$  treatment (Fig. 7E). This time was selected based on our time course western blot data showing heightened CITED1 expression in unmodified RAW264.7 cells at this time (Fig. 1C). As expected, loss of CITED1 expression reversed the increased expression of numerous ISGs observed in CITED1 overexpressing cells (Table S1), including the ten genes featured in Fig. 4B. To verify this result, the change in mRNA levels between IFN $\gamma$ -treated scramble control and CITED1-null cells for this same 10-gene set were measured by qRT-PCR. Here, a statistically significant decrease in expression was seen in the CITED1-null cells for all genes except *Cd52* (Fig. 7F). GO analysis

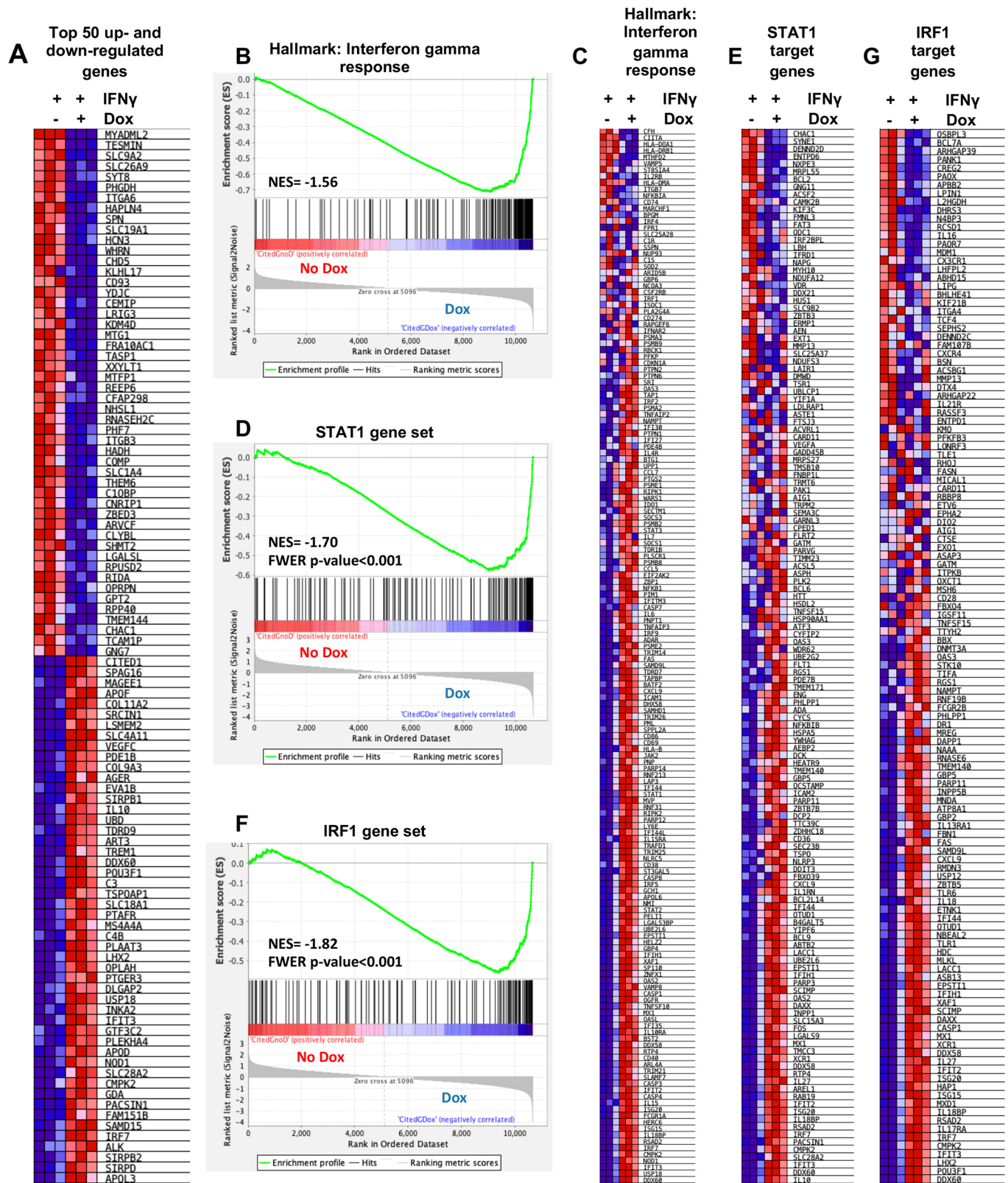


**Fig. 6. CITED1 modulates the expression of STAT1 and IRF1 target genes.** GSEA analysis was performed using the transcriptome profiling dataset described in Fig. 4A. (A) Heatmap of the top 50 up- and down-regulated genes in IFN $\gamma$ -stimulated cells with and without dox-induced CITED1 expression. (B,C) GSEA hallmark analysis of the 'Interferon gamma response' presented as (B) an enrichment score plot with NES and (C) heatmap. (D–G) The same dataset was used together with custom target gene sets to measure the effect on (D,E) STAT1 and (F,G) IRF1 regulated genes and is presented as heatmaps and enrichment score plots. For the analysis using custom target gene sets, a familywise-error rate (FWER) score <0.05 was considered significant. For all heatmaps, red and blue indicate increased and decreased expression, respectively.



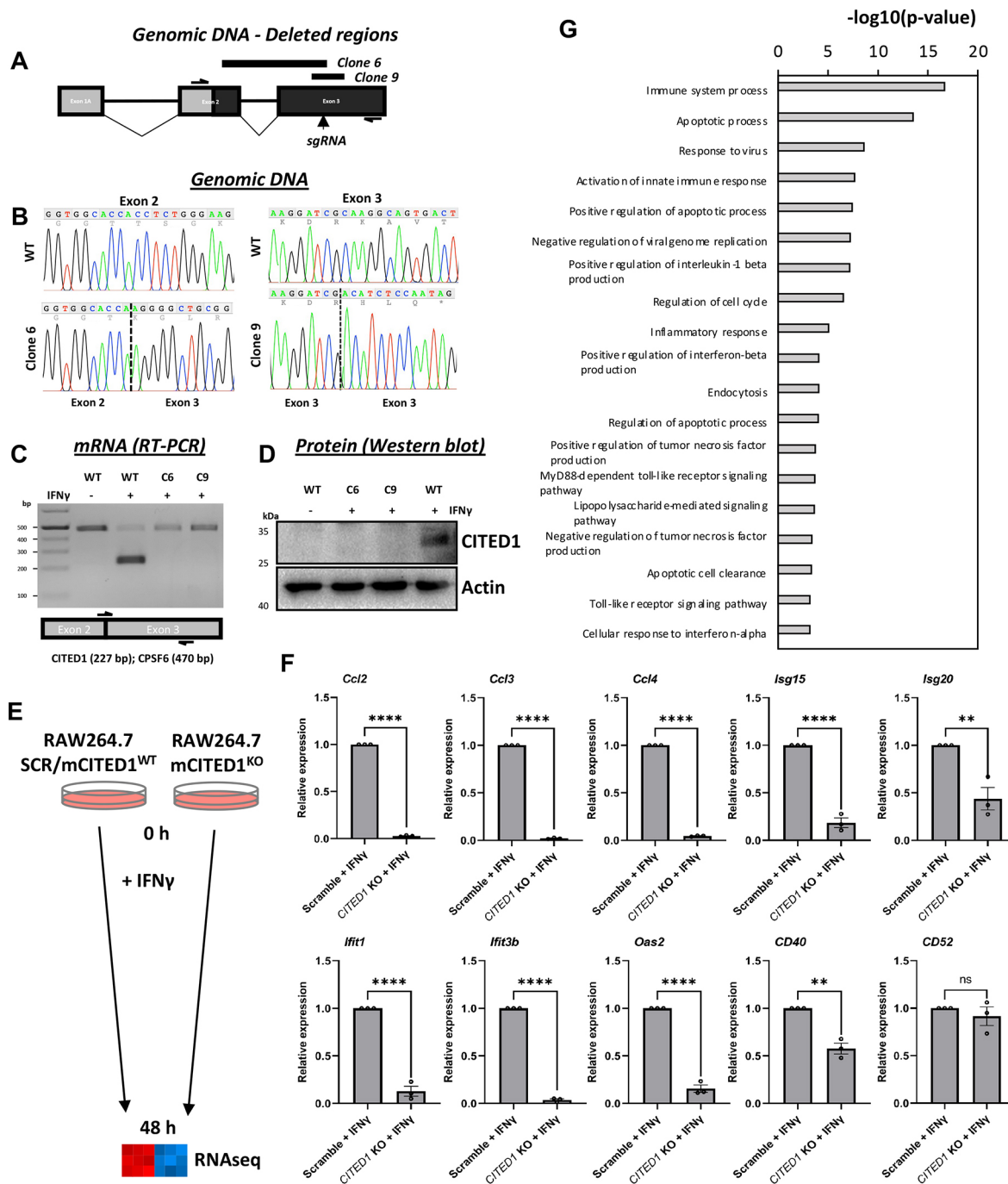


**Fig. 7. Downregulation of ISGs in CITED1 KO cells.** (A) Map of murine *Cited1* gene structure showing protein coding regions of exons (solid black) and the region targeted by an sgRNA to produce knockout (KO) cells (vertical arrow). The region between the horizontal primer arrows was amplified and subjected to Sanger sequencing to characterize INDELs in edited clonal cells. Deletions resulting in frame shifts were identified in clones 6 and 9 (C6 and C9). The regions of genomic DNA deleted for both clones are represented by the solid black lines above the gene map. (B) DNA chromatographs covering the edited region of the *Cited1* gene in clones 6 and 9 (bottom row) and wild-type (WT) cells (top row). (C,D) To confirm loss of both *Cited1* gene expression, CITED1 KO clones and wild type RAW264.7 control cells were incubated with or without IFN $\gamma$  for 24 h. (C) *Cited1* mRNA expression was measured by multiplex RT-PCR using primers for *Cited1* and *CPSF6* as an internal control. The position of *Cited1* forward and reverse primers relative to the exon 2–3 boundary is marked in the diagram below the gel image. (D) CITED1 protein expression was measured by western blotting. A representative experiment out of three repeats is shown for C and D. (E) For the loss-of-function transcriptome profiling experiments, RAW264.7 scramble control (SCR) and CITED1 KO cells were incubated with IFN $\gamma$  for 48 h and total RNA was harvested for RNAseq. (F,G) For the experiment described in E, a selection of DEGs were validated by qRT-PCR (F), and (G) GO analysis was performed in DAVID. A selection of the top BP GO terms are displayed ranked by  $-\log(P\text{-value})$ . For F, error is represented as s.e.m. ( $n=3$ ). \*\* $P<0.01$ ; \*\*\*\* $P<0.0001$ ; ns, not significant (one-way ANOVA followed by a Tukey's multiple comparison test).

of this data set identified BP terms that were consistent with the macrophage response to IFN $\gamma$  (Fig. 7G), many of which were common with the corresponding analysis performed for the

CITED1 overexpression experiment (Fig. 4C). These included 'response to virus', 'inflammatory response' and 'positive regulation of tumor necrosis factor production'. Viewed

collectively, these data indicate that overexpression and loss of CITED1 are impacting an overlapping set of genes, suggesting that it has a genuine role in the regulation of the transcriptional response to IFN $\gamma$  and functions primarily as a positive regulator of genes regulated by STAT1 and IRF1 in this context.

To confirm that loss of CITED1 expression negatively impacted the overall transcriptional response to IFN $\gamma$ , the same transcriptome dataset was reanalyzed using GSEA. Consistent with our initial analysis, a positive NES score was reported for the hallmark 'Interferon gamma response' gene set, indicating that this phenotype was more closely associated with the control than the CITED1-null cells (Fig. S1A,B). Positive NES scores were also obtained for analysis using the custom STAT1 (Fig. S1C,D) and IRF1 gene lists (Fig. S1E,F), which is the opposite to what was observed for the corresponding gain-of-function experiments (Fig. 6).

## DISCUSSION

In this study, we show for the first time that *Cited1* is an IFN $\gamma$ -responsive gene (Fig. 1A,B) with CITED1 protein functioning as a positive regulator of select ISGs (Fig. 8). In this regard, it is functionally distinct from the closely related CITED2, a well-characterized suppressor of myeloid proinflammatory gene

expression (Freedman et al., 2003; Kim et al., 2018; Leung et al., 1999; Lou et al., 2011; Pong Ng et al., 2020; Zafar et al., 2021). This antagonistic relationship between members of transcription factor and co-regulator families is relatively common, with this case being somewhat reminiscent of that seen in the Kruppel-like Factor (KLF) family of transcriptional factors, which also participate in the control of macrophage-mediated inflammation. Among these, Klf2 is largely anti-inflammatory, whereas Klf6 enhances macrophage proinflammatory gene expression (Kim et al., 2016; Nayak et al., 2013).

Although the mechanism driving the contrasting effects of these two CITED proteins is currently unclear, it likely stems from their differing interactions with CBP/p300. CITED2 suppresses the activity of proinflammatory transcriptional regulators, including the STATs, p53-containing NF- $\kappa$ B and HIF-1 $\alpha$  (Kim et al., 2018; Lou et al., 2011; Pong Ng et al., 2020; Zafar et al., 2021), by preventing these proteins from recruiting CBP/p300 to cis-regulatory sites. Here, it acts as a competitive inhibitor, interacting with the N-terminal CH1 domain of CBP/p300, the same region used for docking with these transcription factors (Berlow et al., 2017; Bhattacharya et al., 1999; Freedman et al., 2003; Wojciak et al., 2009). Although CITED1 also associates with the CH1 domain in *in vitro* immunoprecipitation assays, it shows a strong preference for the CH2 domain, located within a central portion of CBP/p300 that contains HAT activity (Yahata et al., 2000). Although this has not been tested, it is conceivable that CITED1 binding via CH2 might still permit the formation of CBP/p300 complexes with proinflammatory transcription factors that dock via CH1. If this is the case, it might even stabilize these complexes by simultaneously interacting with both proteins or stimulating conformational changes in CBP/p300 that enhance transcription factor binding. As an alternative explanation, a feedback relationship between *Cited1* and *Cited2*, as is seen for other gene families (e.g. feedback between p53 and transactivation-deficient isoforms of its homologs, p63 and p73; Grob et al., 2001; Waltermann et al., 2003), could at least partially account for these results. For example, inhibition of *Cited2* gene expression or CITED2–CBP/p300 binding by CITED1 could indirectly result in enhanced ISG expression. However, these possibilities were not supported by the data; no change in *Cited2* expression was detected in our transcriptome profiling studies, and increased CITED2 protein expression was not detected in the CITED1-null cells (data not shown).

In this study, we also show that *Cited1* and *Cited2* exhibit contrasting responses to proinflammatory stimuli. *Cited1* is transcriptionally silent in the absence of stimuli and is only expressed in cells incubated with IFN $\gamma$  for  $\geq 24$  h (Fig. 1A,B). In this way, *Cited1* does not participate in the regulation of basal STAT1-regulated gene expression and its delayed expression prevents it from affecting the early phases of an IFN $\gamma$  response. Rather, it enhances the expression of IFN $\gamma$ -responsive genes at later timepoints. By contrast, we and others show that *Cited2* is constitutively expressed in macrophages (Fig. 1D; Kim et al., 2018), and likely functions to suppress inappropriate proinflammatory gene expression in the absence of stimulus and limit it in the presence of persistent inflammatory signals. Although there is disagreement in the literature concerning the effects of proinflammatory stimuli on *Cited2* expression (Kim et al., 2018; Lou et al., 2011), these data support a model where *Cited2* is transiently downregulated within 6 h post-IFN $\gamma$  treatment, possibly to disinhibit or permit the initial phases of STAT1- and IRF1-directed gene expression (Fig. 1D).

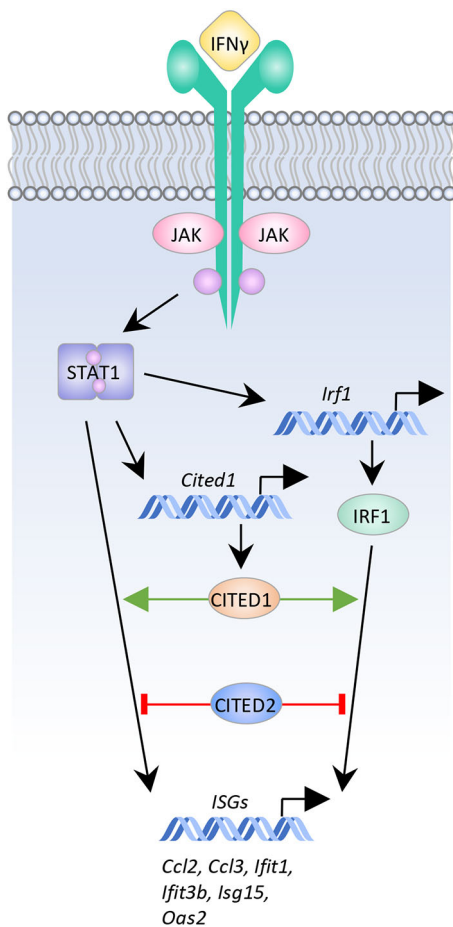


**Fig. 8. CITED1 as a regulation of ISG expression.** IFN $\gamma$ -stimulated activation of STAT1 promotes expression of IRF1. STAT1 and IRF1 operate in concert to increase the expression of numerous ISGs. Data from the current study shows that IFN $\gamma$  stimulation also increases expression of *Cited1* in a STAT1-dependent manner. Unlike CITED2, which represses ISG expression, CITED1 proteins increase the expression of select ISGs.

Regarding the regulation of *Cited1* itself, our data clearly show that it is downstream of STAT1. Computational promoter analysis indicates that the *Cited1* promoter contains both STAT1 and IRF1 cis-regulatory sites (Fig. 2B), which suggests several plausible models for its regulation; it could be regulated by either transcription factor independently, or it could belong to a large subset of ISGs, including *Gbp2*, *Lmp2* and *Socs1*, that are co-regulated by both (Abou El Hassan et al., 2017; Chatterjee-Kishore et al., 1998; Ramsauer et al., 2007). A comprehensive analysis of ISG promoters has shown that relatively few are regulated by STAT1 alone, with STAT1 binding co-occurring with IRF1 most of the time, although IRF1 binding frequently occurs alone (Abou El Hassan et al., 2017). Given that STAT1 drives *Irf1* expression as part of the first wave of ISG transcription (Schroder et al., 2004), co-regulation of *Cited1* by both transcription factors would constitute a coherent feed-forward loop. This mode of regulation serves as a signaling filter for transient stimuli, permitting expression of the target gene only if the activating signal persists for an extended period of time, allowing for the accumulation of both transcriptional regulators. Although feed-forward loops generate delays in target gene expression (Mangan and Alon, 2003), this is unlikely to explain the timing of *Cited1* transcription, which occurs at 24–48 h post-IFN $\gamma$  treatment, as IRF1 is expressed relatively quickly – as part of the first wave of ISG expression – plateauing at ~6 h post-IFN $\gamma$  treatment in RAW264.7 cells (Guinn and Petro, 2019). This suggests that regulation of the *Cited1* gene is more complex and might require additional changes, such as post-translational modifications of STAT1 and IRF1 proteins, other transcriptional regulators or changes to the *Cited1* promoter–chromatin context occurring at later times.

In addition to RNA-level control, this study provides evidence that CITED1 is regulated through altered subcellular localization. In contrast to CITED2, which is reportedly a constitutively nuclear protein (Chou et al., 2012; Lou et al., 2011), ectopic EYFP–CITED1 proteins are predominantly cytosolic in unstimulated macrophages, but accumulate in the nucleus post-IFN $\gamma$  treatment. As a transcriptional co-regulator that operates by controlling the interactions of transcription factors with CBP/p300, the cytosolic sequestration of CITED1 in the absence of stimulus might function as an additional check on its activity, much as it does with other transcription factors, such as NF- $\kappa$ B and NF-AT (Nelson et al., 2004; Ruff and Leach, 1995).

Although the mechanisms regulating CITED1 subcellular localization in macrophages are unclear, the leucine-rich nuclear export signal located in the CR2 domain of CITED1 is likely responsible for the net cytosolic distribution of the protein in unstimulated cells (Shi et al., 2006). How IFN $\gamma$ -stimulation promotes the nuclear accumulation of CITED1 is less obvious, but mechanistic data in other systems might prove instructive. In the osteoblastic cell line MC3T3-E1, PTH stimulation promotes nuclear translocation of CITED1 (Lin et al., 2014). This requires PKC-dependent phosphorylation of CITED1 on S79, which is necessary but not sufficient for nuclear translocation of CITED1. In the current experiments, endogenous CITED1 proteins appeared as at least two bands on western blots (Figs 1C and 2F), suggesting that the protein is also phosphorylated in macrophages. IFN $\gamma$  also stimulated increased phosphorylation of a pre-existing pool of ectopic CITED1 in these cells. Given that IFN $\gamma$  also stimulates PKC activity (Becton et al., 1985; Hamilton et al., 1985), it seems plausible that a similar mechanism to that observed in PTH-stimulated osteoblastic cells might be responsible for CITED1 translocation in macrophages. As a potential caveat, S79 is not conserved in the human version of the protein, so the overall importance of this site is questionable.

It is also possible that the phosphorylation detected in these studies might regulate CITED1 activity in other ways. In addition to S79, murine CITED1 contains five other putative serine phosphorylation sites (S17, S67, S69, S73 and S147; NetPhos-3.1 analysis, phosphorylation site scores >0.90), all of which are conserved between the human and mouse CITED1 sequences (human equivalents are S16, S63, S67, S71 and S137). Shi et al. have shown that all five sites must be ablated to prevent the appearance of partially and hyper-phosphorylated CITED1 species on western blots as HEK293 cells transition through S-phase and mitosis, respectively (Shi et al., 2006). Phospho-mimetic mutants where all five serine residues were mutated to glutamic acid had reduced p300-binding activity and were less able to enhance Smad4-dependent gene expression. This raises the possibility that the phosphorylated CITED1 species detected in the current experiments might also have reduced activity. Future studies mapping the sites of IFN $\gamma$ -stimulated phosphorylation and measuring the effect of these post-translational modifications on the subcellular localization and ability of the protein to modulate the expression of ISGs will provide clarity on this issue.

In closing, our use of a dual gain- and loss-of-function approach has allowed us to identify candidate CITED1-regulated genes with a high degree of confidence. These include members of gene families that are fundamental to the macrophage IFN $\gamma$ -response, such as the C-C motif chemokine family genes, *Ccl2* and *Ccl3*, well-characterized regulators of immune cell migration and inflammation (Mantovani et al., 2004), and also members of the Isg (*Isg15* and *Isg20*) and Ifit (*Ifit1* and *Ifit3b*) gene families. Both the Isg and Ifit family of genes encode proteins that enhance the anti-viral activity of macrophages, but do so by very different mechanisms. The Ifit proteins act as ubiquitin-like modifiers that restrict viral replication in host cells (Fensterl and Sen, 2015), whereas ISG proteins enhance macrophage polarization and nitric oxide production in response to viral infection (Baldanta et al., 2017). Although these data provide important clues to the biological role of CITED1 in innate immune function, a more accurate and holistic view must await future *in vivo* studies. In the meantime, this study points to a greater level of complexity in the control of JAK-STAT signaling and the roles played by the CITED family of proteins in this.

## MATERIALS AND METHODS

### Mammalian cell culture

RAW264.7 macrophage-like cells were obtained from the ATCC (Manassas, VA) and were cultured in DMEM supplemented with 10% FBS, 25 mM HEPES, 1% penicillin and streptomycin, and 50  $\mu$ g/ml gentamicin (all from Sigma-Aldrich). Lenti-X 293 T packaging cells were obtained from Takara-Clontech and were cultured in DMEM supplemented with 10% tetracycline-free FBS (Takara-Clontech), 200 mM L-glutamine, 1 mM sodium pyruvate, and 100 units/ml penicillin and streptomycin. All cell lines were maintained at 37°C in a humidified 5% CO $_2$  atmosphere. For all western blotting, qRT-PCR and RNA sequencing experiments, cells were seeded in six-well plates (Thermo Fisher Scientific) at a density of  $1.5 \times 10^5$  cells/well in 2 ml of medium and grown to ~80% confluency prior to treatment with the indicated reagents. Unless specified otherwise, recombinant murine IFN $\gamma$  (Biolegend, San Diego, CA) was used at a final concentration of 200 U/ml, doxycycline (Thermo Fisher Scientific, Waltham, MA) at 100 ng/ml, and LPS (MilliporeSigma, Burlington, MA) at 100 ng/ml. For treatments lasting longer than 24 h, the medium, cytokines and compounds were replaced at 24-h intervals.

### Plasmids and lentiviral constructs

The pINDUCER20-mCITED1 lentiviral construct was produced by amplifying the full-length murine CITED1 coding sequence from



pCDNA3-Flag-mCITED1 (a kind gift from Mark P. de Caestecker, VUMC, Nashville, USA) and recombining it into the pENTR Gateway donor vector (Addgene #17398) using an In-Fusion ligase-independent cloning kit (Takara-Clontech). The murine CITED1 sequence was then subcloned into the pINDUCER20 lentiviral vector [a kind gift from the Weissmiller laboratory, MTSU, Murfreesboro, USA; originally sourced from the Elledge laboratory (Meerbrey et al., 2011)] using an LR Clonase® II reaction (Life Technologies). The pINDUCER20-EYFP-mCITED1 lentiviral construct was produced by amplifying the full-length murine CITED1 coding sequence from pCDNA3-Flag-mCITED1 and subcloning it into pEYFP-C1 (Takara/Clontech) in-frame with the EYFP-coding sequence. The complete EYFP-mCITED1 sequence was recombined into the pENTR Gateway donor vector using an In-Fusion ligase-independent cloning kit then subcloned into the pINDUCER20 lentiviral vector. The fidelity of all plasmid constructs was verified using by Sanger sequencing (Eurofins Genomics) prior to use in experiments. Lentiviral constructs encoding the Cas9 enzyme and a gRNA were obtained from VectorBuilder, USA. The sequences (5' to 3') of gRNAs targeting murine genes were as follows: *Cited1*, TACCCGGGGGTCACCGCAA; *Stat1*, GTTGGGCGGTCCCCGATGC, and non-targeting 'scramble' gRNA GTGTAGTTCGACCATTCGTG.

### Lentiviral transductions

Lentiviral constructs were packaged by transfection in to Lenti-X 293T cells using a Lenti-X™ Packaging Single Shots kit. Viral supernatants were concentrated and tested for the presence of viral particles using Lenti-X GoStix. The concentrated lentiviral supernatants were used to transduce RAW264.7 cells by spinoculation in the presence of polybrene. Transduced cells were selected by growth in 500 µg/ml G418 (Thermo Fisher Scientific), and then clonal lines were produced by dilution plating. Loss of gene expression was confirmed using a combination of western blotting and RT-PCR. All Lenti-X products were obtained from Takara-Clontech.

### Immunoblotting

For immunoblotting experiments, cells were lysed in RIPA buffer containing protease and phosphatase inhibitors (Sigma). For λ protein phosphatase (λPP) assays, cells were lysed in 1% Triton X-100 in buffer without phosphatase inhibitors. The protein concentration of the samples was determined by BCA assay and normalized by dilution with the appropriate lysis buffer. To dephosphorylate proteins samples, ~50 µg of protein were incubated with 20 units of λPP (NEB, USA) for 30 min. All samples were boiled in 1× Laemmli buffer and resolved by SDS-PAGE and visualized by western blotting. Uncropped western blot images are included as Fig. S2.

### Antibodies

The primary antibodies used for western blotting experiments and their dilutions were as follows: β-actin (A2066, Sigma; 1:5000), IRF-1 (D5E4, 8478S, Cell Signaling Technology; 1:1000), MSG-1 (CITED1; D-7, sc-393585, Santa Cruz Biotechnology; 1:500) and STAT1 (D1K9Y, 14994T, Cell Signaling Technology; 1:1000). Primary antibody binding was detected using mouse anti-rabbit IgG-horseradish peroxidase (HRP; sc-2357, Santa Cruz Biotechnology; 1:5000) or anti-mouse m-IgGkappa binding protein (BP)-HRP (sc-516102, Santa Cruz Biotechnology; 1:5000), as appropriate. Membranes were incubated with standard enhanced chemiluminescent (ECL) reagents or SuperSignal West Atto (Pierce/Thermo Fisher Scientific), and bands were visualized using a ChemiDoc MP Imaging System with Image Lab Software (Bio-Rad, Hercules, CA).

### RNA extraction and RNA sequencing

Total RNA was extracted using RNeasy Mini Kits (Qiagen), according to the manufacturer's instructions with genomic DNA removed from samples using a Message Clean kit (GenHunter, Nashville, USA). Clean RNA was resuspended in 10 µl diethyl pyrocarbonate (DEPC)-treated water and shipped to Novogene (Sacramento, USA). Here, RNA quality was appraised using an Agilent 2100 Bioanalyzer and samples with an acceptable RNA integrity number were used for cDNA library production and RNA

sequencing using the HiSeq 2500 system to produce 150 bp transcriptome paired-end reads.

### Analysis of RNA sequencing data

Quality checks of fastq RNAseq data files were performed using FastQC (version 0.11.5; see <http://www.bioinformatics.babraham.ac.uk/projects/fastqc/>). Based on the data quality, no file trimming was necessary. Reads were aligned to the version 38 mouse genome using STAR aligner (version 2.5.3a; Dobin et al., 2013). Scaffolding was provided by the mouse reference genome annotation (version 39.90, Cunningham et al., 2019) in the CyVerse Discovery Environment (Merchant et al., 2016). In the Galaxy platform (Robinson et al., 2010), a read count table was generated from the bam output from STAR and the same mouse genome annotation using FeatureCounts (Liao et al., 2014) and multi-join (<https://github.com/bgruening/galaxytools>). The resultant read counts were imported into R software, and samples were clustered based on their whole genome gene expression profile using EdgeR (Robinson et al., 2010), as described in Loraine et al. (2015). To evaluate samples for inclusion or exclusion, the data were displayed as a multi-dimensional scale plot. As all samples per condition clustered with their replicate pool ( $n=3$ ), they were all used to construct transcript annotations. To make pairwise comparisons for differentially expressed genes (DEGs) among replicate groups, CuffDiff2 (version 2.2.1; Trapnell et al., 2013) was used with the same mouse genome annotation and genome files. From the pairwise comparisons, DEGs with fold change  $\geq 2.0$  and  $q \leq 0.05$  were considered biologically relevant and statistically significant. Gene ontology (GO) analysis was performed in Database for Annotation, Visualization, and Integrated Discovery (DAVID) 2021 bioinformatics resource tool (version Dec. 2021; Huang et al., 2009a,b). GO terms were ranked and plotted as  $-\log(P\text{-value})$ . For *Cited1* read visualization, bam output files (from STAR), the mouse genome file and the mouse genome annotation were loaded into the Integrated Genome Viewer, which was searched for *Cited1* to display its gene structure with read depth.

Gene set enrichment analysis (GSEA) was performed using GSEA software (version 4.2.3; Mootha et al., 2003; Subramanian et al., 2005). Read counts derived from STAR output (Dobin et al., 2013) were imported into R software and the SARTools R package, DESeq2 version (version 1.7.4; Varet et al., 2016) was used to produce normalized read counts per experiment per sample. As recommended for GSEA from RNA sequencing experiments (Subramanian et al., 2005), genes with no counts in any sample were removed, along with low-expressing genes (mean or geometric mean  $< 10$  reads across all samples). As recommended in the GSEA user guide (<https://www.gsea-msigdb.org/gsea/doc/GSEAUUserGuideFrame.html>), a false discovery rate (FDR) cut of 25% was used for hallmark gene set analysis. STAT1 and IRF1 target gene enrichment analysis was performed in GSEA using custom gene lists assembled by the Mahabeshwar laboratory from data published in Langlais et al. (2016) and Semper et al., 2014 (Langlais et al., 2016; Semper et al., 2014), and has previously been used to measure the effects of *Cited2* loss on STAT1- and IRF1-regulated gene expression (Zafar et al., 2021). For this analysis, a family-wise error rate (FWER)  $< 0.05$  cut-off was used to determine whether a gene set was significantly enriched.

### RT-PCR

For both reverse transcriptase chain reaction (RT-PCR) and quantitative RT-PCR (qRT-PCR) experiments, RNA (isolated as described above) was reverse transcribed to produce cDNA libraries using Maxima H Minus Reverse Transcriptase in the presence of dNTPs, oligo(dT) primers and RiboLock RNase inhibitor (Thermo Fisher Scientific). RT-PCR was performed as a multiplex amplification reaction, using primers for *Cited1* and *Cpsf6* as an internal control. PCR products were resolved on 2% agarose gels containing ethidium bromide and visualized under UV illumination. For qRT-PCR the indicated cDNAs of interest were amplified using PerfeCTa SYBR Green FastMix (Quantabio) in a CFX Opus 96 Real-Time PCR Instrument (Bio-Rad). Normalization was performed using two reference genes (*Cyc1* and *Actb*). Primers were designed such that at least one primer for each pair spanned an exon-exon boundary and produced a product size between 70 and 150 bp. The sequences (5' to 3') of primer pairs

used were as follows: *Actb*, F, CACTGTGCGAGTCGCGTCC, R, TCATC-CATGGCGAACTGGTG; *Ccl2*, F, CAGATGCAGTTAACGCCCA, R, TGAGCTTGGTGACAAAACTACAG; *Ccl3*, F, CCAAGTCTTCTCA-GCGCCATA, R, TCTCTTAGTCAGGAAAATGACACC; *Ccl4*, F, CTG-TGCAAACCTAACCCCGA, R, AGGGTCAGAGCCCATTGGT, *Cd40*, F, TTGTTGACAGCGGTCCATCT, R, TTCCTGGCTGGCACAAATCA; *Cd52*, F, CAAAGCTGCTACAGAGCCCA, R, CCAAGGATCCTGTTG-TATCTGAAT; *Cited1*, F, CTGCCACCGATTATCGGACTT, R, CTCCT-GGTTGGCATCCTCCTT; *Cited2*, F, GCAAAGACGGAAGGACTGGA, R, CGTAGTGTATGTGCTCGCCC; *Cpsf6*, F, TTACACTGGGAAGA-GAATCGC, R, CTGGAAAAGGTGGAGGTGG; *Cyc1*, F, CTAACCT-GAGGCTGCAAGA, R, GCCAGTGAGCAGGGAAAATA; *Ifit1*, F, TC-TGCTCTGCTGAAAACCCA, R, CACCATCAGCATTTCTCTCCCAT; *Ifit3b*, F, CCTTCTGCCAAGGATTGCT, R, TGTGATCAAAAGGTG-GTCTGTGA; *Isg15*, F, TCTGACTGTGAGAGCAAGCAG, R, CCTT-TAGGTCCCAGGCCATT; *Isg20*, F, TGAAGCCAGGCTAGAGATCC, R, AGGGCATTGAAGTCGTGCTT; and *Oas2*, F, GCCTTGAAAGTGC-CAGTACC, R, CCTTGGTCTGCCACAAGAT.

### Genotype-tissue expression analysis

The online Genotype-Tissue Expression (GTEx) resource was employed to compare the expression of human *Cited* family members across 54 non-diseased tissues from ~1000 individuals. The following Ensembl gene IDs were used for the analysis ENSG00000125931 (*Cited1*), ENSG00000164442 (*Cited2*) and ENSG00000179862 (*Cited4*).

### Promoter analysis

Putative transcription factor binding sites in the *Mus musculus Cited1* promoter were identified using the Eukaryotic Promoter Database (EPD; Swiss Institute of Bioinformatics) with the Jasper core 2018 vertebrates transcription factor motif library (Dreos et al., 2017). The promoter (NCBI Reference Sequence: NM\_007709) was scanned from -2000 to 100 bp relative to the transcriptional start site with a cut-off (*P*-value) of 0.001.

### Fluorescence microscopy

Clonal RAW264.7 cells stably transduced with pINDUCER20-EYFP-CITED1 were plated at  $1.5 \times 10^5$ /dish with 2 ml medium in 35 mm glass-bottom dishes (Cellvis, USA) and incubated with 100 ng/ml doxycycline to induce EYFP-CITED1 protein expression prior to IFN $\gamma$  treatment for the indicated periods. Cells were stained with 2.5  $\mu$ g/ml Hoechst 33342 (MilliporeSigma) 30 min prior to imaging using a Zeiss LSM700 confocal laser scanning microscope equipped with a Plan-Apochromat 63 $\times$  magnification/1.40 numerical aperture oil immersion DIC M27 objective lens and controlled using Zen software (Zeiss). EYFP fluorescence was excited using a 488 nm laser. Hoechst 33342 was excited using a 405 nm laser and detected through a 490 nm short-pass filter. To calculate nuclear: cytoplasmic EYFP-CITED1 ratios, mean nuclear and cytoplasmic fluorescence intensity measurements were made using Fiji software (Schindelin et al., 2012), and these data were exported to Excel software.

### Statistical analysis

All experiments were performed as three discrete biological repeats unless otherwise stated. Statistical analyses were performed in GraphPad Prism 7 (GraphPad, USA) using the tests indicated in the figure legends.

### Acknowledgements

We thank the Mahabeshwar lab (Case Western Reserve University) for providing assistance with the GSEA analysis using STAT1 and IRF1 target gene sets. Thanks also to the de Caestecker lab (Vanderbilt University) for providing the murine CITED1 expression plasmid.

### Competing interests

The authors declare no competing or financial interests.

### Author contributions

Conceptualization: D.E.N.; Methodology: A.S., E.E.M., R.L.S.-T., D.E.N.; Software: R.L.S.-T.; Validation: D.E.N.; Formal analysis: A.S., M.E.L.H., S.G., J.M., R.L.S.-T., D.E.N.; Investigation: A.S., M.E.L.H., S.G., J.M., H.K., G.E.M., R.L.S.-T., D.E.N.;

Resources: R.L.S.-T., D.E.N.; Data curation: A.S., S.G., R.L.S.-T., D.E.N.; Writing - original draft: D.E.N.; Writing - review & editing: E.E.M., R.L.S.-T., D.E.N.; Visualization: A.S., M.E.L.H., J.M., H.K., R.L.S.-T., D.E.N.; Supervision: E.E.M., R.L.S.-T., D.E.N.; Project administration: E.E.M., R.L.S.-T., D.E.N.; Funding acquisition: E.E.M., R.L.S.-T., D.E.N.

### Funding

This work was supported by funds from the National Institutes of Health (NIAID 1R15AI135826-01) to D.E.N., E.E.M. and R.L.S.-T., and the Molecular Biosciences (MOBI) doctoral program at Middle Tennessee State University (MTSU) to D.E.N. and A.S. G.E.M., M.E.L.H., and H.K. received funding through the Undergraduate Research Experience and Creative Activity (URECA) Program at MTSU. Deposited in PMC for release after 12 months.

### Data availability

The original RNA sequencing files have been deposited in NCBI GEO under the accession numbers GSE217961 and GSE218356 for the CITED1 overexpression and knockout experiments, respectively.

### Peer review history

The peer review history is available online at <https://journals.biologists.com/jcs/lookup/doi/10.1242/jcs.260529.reviewer-comments.pdf>

### References

- Abou El Hassan, M., Huang, K., Eswara, M. B., Xu, Z., Yu, T., Aubry, A., Ni, Z., Livne-Bar, I., Sangwan, M., Ahmad, M. et al. (2017). Properties of STAT1 and IRF1 enhancers and the influence of SNPs. *BMC Mol. Biol.* **18**, 6. doi:10.1186/s12867-017-0084-1
- Aguiar, K. M. and Gibson, G. W. (2000). Differing requirement for inducible nitric oxide synthase activity in clearance of primary and secondary *Cryptococcus neoformans* infection. *Med. Mycol.* **38**, 343-353. doi:10.1080/mmy.38.5.343.353
- Alexander, W. S., Starr, R., Fenner, J. E., Scott, C. L., Handman, E., Sprigg, N. S., Corbin, J. E., Cornish, A. L., Darwiche, R., Owczarek, C. M. et al. (1999). SOCS1 is a critical inhibitor of interferon  $\gamma$  signaling and prevents the potentially fatal neonatal actions of this cytokine. *Cell* **98**, 597-608. doi:10.1016/S0092-8674(00)80047-1
- Andrews, J. E., O'Neill, M. J., Binder, M., Shioda, T. and Sinclair, A. H. (2000). Isolation and expression of a novel member of the CITED family. *Mech. Dev.* **95**, 305-308. doi:10.1016/S0925-4773(00)00362-2
- Baldanta, S., Fernandez-Escobar, M., Acin-Perez, R., Albert, M., Camafeita, E., Jorge, I., Vazquez, J., Enriquez, J. A. and Guerra, S. (2017). ISG15 governs mitochondrial function in macrophages following vaccinia virus infection. *PLoS Pathog.* **13**, e1006651. doi:10.1371/journal.ppat.1006651
- Becton, D. L., Adams, D. O. and Hamilton, T. A. (1985). Characterization of protein kinase C activity in interferon  $\gamma$  treated murine peritoneal macrophages. *J. Cell. Physiol.* **125**, 485-491. doi:10.1002/jcp.1041250318
- Berlow, R. B., Dyson, H. J. and Wright, P. E. (2017). Hypersensitive termination of the hypoxic response by a disordered protein switch. *Nature* **543**, 447-451. doi:10.1038/nature21705
- Beyer, M., Mallmann, M. R., Xue, J., Staratschek-Jox, A., Vorholt, D., Krebs, W., Sommer, D., Sander, J., Mertens, C., Nino-Castro, A. et al. (2012). High-resolution transcriptome of human macrophages. *PLoS One* **7**, e45466. doi:10.1371/journal.pone.0045466
- Bhattacharya, S., Michels, C. L., Leung, M. K., Arany, Z. P., Kung, A. L. and Livingston, D. M. (1999). Functional role of p35srj, a novel p300/CBP binding protein, during transactivation by HIF-1. *Genes Dev.* **13**, 64-75. doi:10.1101/gad.13.1.64
- Bluyssen, H. A., Vlietstra, R. J., Faber, P. W., Smit, E. M., Hagemeijer, A. and Trapman, J. (1994). Structure, chromosome localization, and regulation of expression of the interferon-regulated mouse Ifi54/Ifi56 gene family. *Genomics* **24**, 137-148. doi:10.1006/geno.1994.1591
- Boyle, S., Shioda, T., Perantoni, A. O. and De Caestecker, M. (2007). Cited1 and Cited2 are differentially expressed in the developing kidney but are not required for nephrogenesis. *Dev. Dyn.* **236**, 2321-2330. doi:10.1002/dvdy.21242
- Braganca, J., Swingle, T., Marques, F. I., Jones, T., Eloranta, J. J., Hurst, H. C., Shioda, T. and Bhattacharya, S. (2002). Human CREB-binding protein/p300-interacting transactivator with ED-rich tail (CITED) 4, a new member of the CITED family, functions as a co-activator for transcription factor AP-2. *J. Biol. Chem.* **277**, 8559-8565. doi:10.1074/jbc.M110850200
- Chatterjee-Kishore, M., Kishore, R., Hicklin, D. J., Marincola, F. M. and Ferrone, S. (1998). Different requirements for signal transducer and activator of transcription 1 $\alpha$  and interferon regulatory factor 1 in the regulation of low molecular mass polypeptide 2 and transporter associated with antigen processing 1 gene expression. *J. Biol. Chem.* **273**, 16177-16183. doi:10.1074/jbc.273.26.16177



- Chen, Y., Haviernik, P., Bunting, K. D. and Yang, Y.-C. (2007). Cited2 is required for normal hematopoiesis in the murine fetal liver. *Blood* **110**, 2889–2898. doi:10.1182/blood-2007-01-066316
- Chou, Y. T., Hsieh, C. H., Chiou, S. H., Hsu, C. F., Kao, Y. R., Lee, C. C., Chung, C. H., Wang, Y. H., Hsu, H. S., Pang, S. T. et al. (2012). CITED2 functions as a molecular switch of cytokine-induced proliferation and quiescence. *Cell Death Differ.* **19**, 2015–2028. doi:10.1038/cdd.2012.91
- Cunningham, F., Achuthan, P., Akanni, W., Allen, J., Amode, M. R., Armean, I. M., Bennett, R., Bhari, J., Billis, K., Boddu, S. et al. (2019). Ensembl 2019. *Nucleic Acids Res.* **47**, D745–D751. doi:10.1093/nar/gky1113
- Decker, T., Kovarik, P. and Meinke, A. (1997). GAS elements: a few nucleotides with a major impact on cytokine-induced gene expression. *J. Interferon Cytokine Res.* **17**, 121–134. doi:10.1089/jir.1997.17.121
- Dobin, A., Davis, C. A., Schlesinger, F., Drenkow, J., Zaleski, C., Jha, S., Batut, P., Chaisson, M. and Gingeras, T. R. (2013). STAR: ultrafast universal RNA-seq aligner. *Bioinformatics* **29**, 15–21. doi:10.1093/bioinformatics/bts635
- Dorrington, M. G. and Fraser, I. D. C. (2019). NF- $\kappa$ B signaling in macrophages: dynamics, crosstalk, and signal integration. *Front. Immunol.* **10**, 705. doi:10.3389/fimmu.2019.00705
- Dreos, R., Ambrosini, G., Perier, R. C. and Bucher, P. (2015). The eukaryotic promoter database: expansion of EPDnew and new promoter analysis tools. *Nucleic Acids Res.* **43**, D92–D96. doi:10.1093/nar/gku1111
- Dreos, R., Ambrosini, G., Groux, R., Cavin Perier, R. and Bucher, P. (2017). The eukaryotic promoter database in its 30th year: focus on non-vertebrate organisms. *Nucleic Acids Res.* **45**, D51–D55. doi:10.1093/nar/gkw1069
- Durbin, J. E., Hackenmiller, R., Simon, M. C. and Levy, D. E. (1996). Targeted disruption of the mouse Stat1 gene results in compromised innate immunity to viral disease. *Cell* **84**, 443–450. doi:10.1016/S0092-8674(00)81289-1
- Fenner, M. H., Parrish, J. E., Boyd, Y., Reed, V., Macdonald, M., Nelson, D. L., Isselbacher, K. J. and Shioda, T. (1998). MSG1 (melanocyte-specific gene 1): mapping to chromosome Xq13.1, genomic organization, and promoter analysis. *Genomics* **51**, 401–407. doi:10.1006/geno.1998.5383
- Fensterl, V. and Sen, G. C. (2015). Interferon-induced Irf proteins: their role in viral pathogenesis. *J. Virol.* **89**, 2462–2468. doi:10.1128/JVI.02744-14
- Fitzgerald, K. A. and Kagan, J. C. (2020). Toll-like receptors and the control of immunity. *Cell* **180**, 1044–1066. doi:10.1016/j.cell.2020.02.041
- Freedman, S. J., Sun, Z.-Y., Kung, A. L., France, D. S., Wagner, G. and Eck, M. J. (2003). Structural basis for negative regulation of hypoxia-inducible factor-1 $\alpha$  by CITED2. *Nat. Struct. Biol.* **10**, 504–512. doi:10.1038/nsb936
- Gill, N., Chenoweth, M. J., Verdu, E. F. and Ashkar, A. A. (2011). NK cells require type I IFN receptor for antiviral responses during genital HSV-2 infection. *Cell. Immunol.* **269**, 29–37. doi:10.1016/j.cellimm.2011.03.007
- Ginhoux, F. and Jung, S. (2014). Monocytes and macrophages: developmental pathways and tissue homeostasis. *Nat. Rev. Immunol.* **14**, 392–404. doi:10.1038/nri3671
- Gongora, C., Degols, G., Espert, L., Hua, T. D. and Mechti, N. (2000). A unique ISRE, in the TATA-less human Isg20 promoter, confers IRF-1-mediated responsiveness to both interferon type I and type II. *Nucleic Acids Res.* **28**, 2333–2341. doi:10.1093/nar/28.12.2333
- Grob, T. J., Novak, U., Maisse, C., Barcaroli, D., Luthi, A. U., Pirnia, F., Hugli, B., Graber, H. U., De Laurenzi, V., Fey, M. F. et al. (2001). Human delta Np73 regulates a dominant negative feedback loop for TAp73 and p53. *Cell Death Differ.* **8**, 1213–1223. doi:10.1038/sj.cdd.4400962
- GTEX Consortium. (2013). The genotype-tissue expression (GTEx) project. *Nat. Genet.* **45**, 580–585. doi:10.1038/ng.2653
- Guinn, Z. P. and Petro, T. M. (2019). Interferon regulatory factor 3 plays a role in macrophage responses to interferon- $\gamma$ . *Immunobiology* **224**, 565–574. doi:10.1016/j.imbio.2019.04.004
- Hamilton, T. A., Becton, D. L., Somers, S. D., Gray, P. W. and Adams, D. O. (1985). Interferon- $\gamma$  modulates protein kinase C activity in murine peritoneal macrophages. *J. Biol. Chem.* **260**, 1378–1381. doi:10.1016/S0021-9258(18)89600-4
- Hardison, S. E., Ravi, S., Wozniak, K. L., Young, M. L., Olszewski, M. A. and Wormley, F. L. Jr. (2010). Pulmonary infection with an interferon- $\gamma$ -producing *Cryptococcus neoformans* strain results in classical macrophage activation and protection. *Am. J. Pathol.* **176**, 774–785. doi:10.2353/ajpath.2010.090634
- Hardison, S. E., Herrera, G., Young, M. L., Hole, C. R., Wozniak, K. L. and Wormley, F. L. Jr. (2012). Protective immunity against pulmonary *Cryptococcus* is associated with STAT1-mediated classical macrophage activation. *J. Immunol.* **189**, 4060–4068. doi:10.4049/jimmunol.1103455
- Howlin, J., McBryan, J., Napoletano, S., Lambe, T., Mcardle, E., Shioda, T. and Martin, F. (2006). CITED1 homozygous null mice display aberrant pubertal mammary ductal morphogenesis. *Oncogene* **25**, 1532–1542. doi:10.1038/sj.onc.1209183
- Hu, X., Herrero, C., Li, W. P., Antoniv, T. T., Falck-Pedersen, E., Koch, A. E., Woods, J. M., Haines, G. K. and Ivashkiv, L. B. (2002). Sensitization of IFN- $\gamma$  Jak-STAT signaling during macrophage activation. *Nat. Immunol.* **3**, 859–866. doi:10.1038/ni828
- Hu, X., Park-Min, K. H., Ho, H. H. and Ivashkiv, L. B. (2005). IFN- $\gamma$ -primed macrophages exhibit increased CCR2-dependent migration and altered IFN- $\gamma$  responses mediated by Stat1. *J. Immunol.* **175**, 3637–3647. doi:10.4049/jimmunol.175.6.3637
- Huang, D. W., Sherman, B. T. and Lempicki, R. A. (2009a). Bioinformatics enrichment tools: paths toward the comprehensive functional analysis of large gene lists. *Nucleic Acids Res.* **37**, 1–13. doi:10.1093/nar/gkn923
- Huang, D. W., Sherman, B. T. and Lempicki, R. A. (2009b). Systematic and integrative analysis of large gene lists using DAVID bioinformatics resources. *Nat. Protoc.* **4**, 44–57. doi:10.1038/nprot.2008.211
- Jablonski, K. A., Amici, S. A., Webb, L. M., Ruiz-Rosado Jde, D., Popovich, P. G., Partida-Sanchez, S. and Guerau-De-Arellano, M. (2015). Novel markers to delineate murine M1 and M2 macrophages. *PLoS One* **10**, e0145342. doi:10.1371/journal.pone.0145342
- Kim, Y.-M., Lee, B.-S., Yi, K.-Y. and Paik, S.-G. (1997). Upstream NF- $\kappa$ B site is required for the maximal expression of mouse inducible nitric oxide synthase gene in interferon- $\gamma$  plus lipopolysaccharide-induced RAW 264.7 macrophages. *Biochem. Biophys. Res. Commun.* **236**, 655–660. doi:10.1006/bbrc.1997.7031
- Kim, G. D., Das, R., Goduni, L., McClellan, S., Hazlett, L. D. and Mahabeleshwar, G. H. (2016). Kruppel-like factor 6 promotes macrophage-mediated inflammation by suppressing B cell leukemia/lymphoma 6 expression. *J. Biol. Chem.* **291**, 21271–21282. doi:10.1074/jbc.M116.738617
- Kim, G. D., Das, R., Rao, X., Zhong, J., Deiuliis, J. A., Ramirez-Bergeron, D. L., Rajagopalan, S. and Mahabeleshwar, G. H. (2018). CITED2 restrains proinflammatory macrophage activation and response. *Mol. Cell. Biol.* **38**, e00452-17. doi:10.1128/MCB.00452-17
- Kranc, K. R., Schepers, H., Rodrigues, N. P., Bamforth, S., Villadsen, E., Ferry, H., Bouriez-Jones, T., Sigvardsson, M., Bhattacharya, S., Jacobsen, S. E. et al. (2009). Cited2 is an essential regulator of adult hematopoietic stem cells. *Cell Stem Cell* **5**, 659–665. doi:10.1016/j.stem.2009.11.001
- Kroger, A., Koster, M., Schroeder, K., Hauser, H. and Mueller, P. P. (2002). Activities of IRF-1. *J. Interferon Cytokine Res.* **22**, 5–14. doi:10.1089/107999002753452610
- Kumatori, A., Yang, D., Suzuki, S. and Nakamura, M. (2002). Cooperation of STAT-1 and IRF-1 in interferon- $\gamma$ -induced transcription of the gp91(phox) gene. *J. Biol. Chem.* **277**, 9103–9111. doi:10.1074/jbc.M109803200
- Langlais, D., Barreiro, L. B. and Gros, P. (2016). The macrophage IRF8/IRF1 regulome is required for protection against infections and is associated with chronic inflammation. *J. Exp. Med.* **213**, 585–603. doi:10.1084/jem.20151764
- Leopold Wager, C. M., Hole, C. R., Wozniak, K. L., Olszewski, M. A. and Wormley, F. L. Jr. (2014). STAT1 signaling is essential for protection against *Cryptococcus neoformans* infection in mice. *J. Immunol.* **193**, 4060–4071. doi:10.4049/jimmunol.1400318
- Leopold Wager, C. M., Hole, C. R., Wozniak, K. L., Olszewski, M. A., Mueller, M. and Wormley, F. L. Jr. (2015). STAT1 signaling within macrophages is required for antifungal activity against *Cryptococcus neoformans*. *Infect. Immun.* **83**, 4513–4527. doi:10.1128/IAI.00935-15
- Leung, M. K., Jones, T., Michels, C. L., Livingston, D. M. and Bhattacharya, S. (1999). Molecular cloning and chromosomal localization of the human CITED2 gene encoding p35srj/Mrg1. *Genomics* **61**, 307–313. doi:10.1006/geno.1999.5970
- Liao, Y., Smyth, G. K. and Shi, W. (2014). featureCounts: an efficient general purpose program for assigning sequence reads to genomic features. *Bioinformatics* **30**, 923–930. doi:10.1093/bioinformatics/btt656
- Liau, N. P. D., Laktuyushin, A., Lucet, I. S., Murphy, J. M., Yao, S., Whitlock, E., Callaghan, K., Nicola, N. A., Kershaw, N. J. and Babon, J. J. (2018). The molecular basis of JAK/STAT inhibition by SOCS1. *Nat. Commun.* **9**, 1558. doi:10.1038/s41467-018-04013-1
- Lin, Z., Feng, R., Li, J., Meng, Y., Yuan, L., Fu, Z., Guo, J., Bringham, F. R. and Yang, D. (2014). Nuclear translocation of CBP/p300-interacting protein CITED1 induced by parathyroid hormone requires serine phosphorylation at position 79 in its 63–84 domain. *Cell. Signal.* **26**, 2436–2445. doi:10.1016/j.cellsig.2014.06.015
- Loraine, A. E., Blakley, I. C., Jagadeesan, S., Harper, J., Miller, G. and Firon, N. (2015). Analysis and visualization of RNA-seq expression data using RStudio, bioconductor, and integrated genome browser. *Methods Mol. Biol.* **1284**, 481–501. doi:10.1007/978-1-4939-2444-8\_24
- Lou, X., Sun, S., Chen, W., Zhou, Y., Huang, Y., Liu, X., Shan, Y. and Wang, C. (2011). Negative feedback regulation of NF- $\kappa$ B action by CITED2 in the nucleus. *J. Immunol.* **186**, 539–548. doi:10.4049/jimmunol.1001650
- Mangan, S. and Alon, U. (2003). Structure and function of the feed-forward loop network motif. *Proc. Natl. Acad. Sci. USA* **100**, 11980–11985. doi:10.1073/pnas.2133841100
- Mantovani, A., Sica, A., Sozzani, S., Allavena, P., Vecchi, A. and Locati, M. (2004). The chemokine system in diverse forms of macrophage activation and polarization. *Trends Immunol.* **25**, 677–686. doi:10.1016/j.it.2004.09.015
- Meerbrey, K. L., Hu, G., Kessler, J. D., Roarty, K., Li, M. Z., Fang, J. E., Herschkowitz, J. I., Burrows, A. E., Ciccio, A., Sun, T. et al. (2011). The pINDUCER lentiviral toolkit for inducible RNA interference in vitro and in vivo. *Proc. Natl. Acad. Sci. USA* **108**, 3665–3670. doi:10.1073/pnas.1019736108



- Meraz, M. A., White, J. M., Sheehan, K. C., Bach, E. A., Rodig, S. J., Dighe, A. S., Kaplan, D. H., Riley, J. K., Greenlund, A. C., Campbell, D. et al. (1996). Targeted disruption of the Stat1 gene in mice reveals unexpected physiologic specificity in the JAK-STAT signaling pathway. *Cell* **84**, 431-442. doi:10.1016/S0092-8674(00)81288-X
- Merchant, N., Lyons, E., Goff, S., Vaughn, M., Ware, D., Micklos, D. and Antin, P. (2016). The iPlant collaborative: cyberinfrastructure for enabling data to discovery for the life sciences. *PLoS Biol.* **14**, e1002342. doi:10.1371/journal.pbio.1002342
- Michalska, A., Blaszczyk, K., Wesoly, J. and Bluyssen, H. A. R. (2018). A positive feedback amplifier circuit that regulates interferon (IFN)-stimulated gene expression and controls type I and type II IFN responses. *Front. Immunol.* **9**, 1135. doi:10.3389/fimmu.2018.01135
- Mootha, V. K., Lindgren, C. M., Eriksson, K. F., Subramanian, A., Sihag, S., Lehar, J., Puigserver, P., Carlsson, E., Ridderstrale, M., Laurila, E. et al. (2003). PGC-1 $\alpha$ -responsive genes involved in oxidative phosphorylation are coordinately downregulated in human diabetes. *Nat. Genet.* **34**, 267-273. doi:10.1038/ng1180
- Murray, P. J. and Smale, S. T. (2012). Restraint of inflammatory signaling by interdependent strata of negative regulatory pathways. *Nat. Immunol.* **13**, 916-924. doi:10.1038/ni.2391
- Murray, P. J., Allen, J. E., Biswas, S. K., Fisher, E. A., Gilroy, D. W., Goerdt, S., Gordon, S., Hamilton, J. A., Ivashkiv, L. B., Lawrence, T. et al. (2014). Macrophage activation and polarization: nomenclature and experimental guidelines. *Immunity* **41**, 14-20. doi:10.1016/j.immuni.2014.06.008
- Nayak, L., Goduni, L., Takami, Y., Sharma, N., Kapil, P., Jain, M. K. and Mahabeleshwar, G. H. (2013). Kruppel-like factor 2 is a transcriptional regulator of chronic and acute inflammation. *Am. J. Pathol.* **182**, 1696-1704. doi:10.1016/j.ajpath.2013.01.029
- Nelson, D. E., Ihekweaba, A. E., Elliott, M., Johnson, J. R., Gibney, C. A., Foreman, B. E., Nelson, G., See, V., Horton, C. A., Spiller, D. G. et al. (2004). Oscillations in NF-kappaB signaling control the dynamics of gene expression. *Science* **306**, 704-708. doi:10.1126/science.1099962
- Ogony, J., Choi, H. J., Lui, A., Cristofanilli, M. and Lewis-Wambi, J. (2016). Interferon-induced transmembrane protein 1 (IFITM1) overexpression enhances the aggressive phenotype of SUM149 inflammatory breast cancer cells in a signal transducer and activator of transcription 2 (STAT2)-dependent manner. *Breast Cancer Res.* **18**, 25. doi:10.1186/s13058-016-0683-7
- Ohtomo, T., Sugamata, Y., Ozaki, Y., Ono, K., Yoshimura, Y., Kawai, S., Koishihara, Y., Ozaki, S., Kosaka, M., Hirano, T. et al. (1999). Molecular cloning and characterization of a surface antigen preferentially overexpressed on multiple myeloma cells. *Biochem. Biophys. Res. Commun.* **258**, 583-591. doi:10.1006/bbrc.1999.0683
- Pine, R., Decker, T., Kessler, D. S., Levy, D. E. and Darnell, J. E. Jr. (1990). Purification and cloning of interferon-stimulated gene factor 2 (ISGF2): ISGF2 (IRF-1) can bind to the promoters of both beta interferon- and interferon-stimulated genes but is not a primary transcriptional activator of either. *Mol. Cell. Biol.* **10**, 2448-2457. doi:10.1128/mcb.10.6.2448-2457.1990
- Pong Ng, H., Kim, G. D., Ricky Chan, E., Dunwoodie, S. L. and Mahabeleshwar, G. H. (2020). CITED2 limits pathogenic inflammatory gene programs in myeloid cells. *FASEB J.* **34**, 12100-12113. doi:10.1096/fj.20200864R
- Qin, X., Chen, H., Tu, L., Ma, Y., Liu, N., Zhang, H., Li, D., Riedl, B., Bierer, D., Yin, F. et al. (2021). Potent inhibition of HIF1 $\alpha$  and p300 interaction by a constrained peptide derived from CITED2. *J. Med. Chem.* **64**, 13693-13703. doi:10.1021/acs.jmedchem.1c01043
- Ramana, C. V., Gil, M. P., Schreiber, R. D. and Stark, G. R. (2002). Stat1-dependent and -independent pathways in IFN- $\gamma$ -dependent signaling. *Trends Immunol.* **23**, 96-101. doi:10.1016/S1471-4906(01)02118-4
- Ramsauer, K., Farlik, M., Zupkovitz, G., Seiser, C., Kroger, A., Hauser, H. and Decker, T. (2007). Distinct modes of action applied by transcription factors STAT1 and IRF1 to initiate transcription of the IFN- $\gamma$ -inducible gbp2 gene. *Proc. Natl. Acad. Sci. USA* **104**, 2849-2854. doi:10.1073/pnas.0610944104
- Robinson, M. D., McCarthy, D. J. and Smyth, G. K. (2010). edgeR: a Bioconductor package for differential expression analysis of digital gene expression data. *Bioinformatics* **26**, 139-140. doi:10.1093/bioinformatics/btp616
- Ronni, T., Matikainen, S., Lehtonen, A., Palvimo, J., Dellis, J., Van Eylen, F., Goetschy, J. F., Horisberger, M., Content, J. and Julkunen, I. (1998). The proximal interferon-stimulated response elements are essential for interferon responsiveness: a promoter analysis of the antiviral MxA gene. *J. Interferon Cytokine Res.* **18**, 773-781. doi:10.1089/jir.1998.18.773
- Ruff, V. A. and Leach, K. L. (1995). Direct demonstration of NFATp dephosphorylation and nuclear localization in activated HT-2 cells using a specific NFATp polyclonal antibody. *J. Biol. Chem.* **270**, 22602-22607. doi:10.1074/jbc.270.38.22602
- Schindelin, J., Arganda-Carreras, I., Frise, E., Kaynig, V., Longair, M., Pietzsch, T., Preibisch, S., Rueden, C., Saalfeld, S., Schmid, B. et al. (2012). Fiji: an open-source platform for biological-image analysis. *Nat. Methods* **9**, 676-682. doi:10.1038/nmeth.2019
- Schroder, K., Hertzog, P. J., Ravasi, T. and Hume, D. A. (2004). Interferon- $\gamma$ : an overview of signals, mechanisms and functions. *J. Leukoc. Biol.* **75**, 163-189. doi:10.1189/jlb.0603252
- Semper, C., Leitner, N. R., Lassnig, C., Parrini, M., Mahlakoiv, T., Rammerstorfer, M., Lorenz, K., Rigler, D., Muller, S., Kolbe, T. et al. (2014). STAT1 $\beta$  is not dominant negative and is capable of contributing to  $\gamma$  interferon-dependent innate immunity. *Mol. Cell. Biol.* **34**, 2235-2248. doi:10.1128/MCB.00295-14
- Shi, G., Boyle, S. C., Sparrow, D. B., Dunwoodie, S. L., Shioda, T. and De Caestecker, M. P. (2006). The transcriptional activity of CITED1 is regulated by phosphorylation in a cell cycle-dependent manner. *J. Biol. Chem.* **281**, 27426-27435. doi:10.1074/jbc.M602631200
- Shioda, T., Fenner, M. H. and Isselbacher, K. J. (1996). msg1, a novel melanocyte-specific gene, encodes a nuclear protein and is associated with pigmentation. *Proc. Natl. Acad. Sci. USA* **93**, 12298-12303. doi:10.1073/pnas.93.22.12298
- Shuai, K. and Liu, B. (2003). Regulation of JAK-STAT signalling in the immune system. *Nat. Rev. Immunol.* **3**, 900-911. doi:10.1038/nri1226
- Sikorski, K., Chmielewski, S., Olejnik, A., Wesoly, J. Z., Heemann, U., Baumann, M. and Bluyssen, H. (2012). STAT1 as a central mediator of IFN $\gamma$  and TLR4 signal integration in vascular dysfunction. *JAKSTAT* **1**, 241-249. doi:10.4161/jkst.22469
- Subramani, A., Griggs, P., Frantzen, N., Mendez, J., Tucker, J., Murriel, J., Sircy, L. M., Millican, G. E., McClelland, E. E., Seipelt-Thiemann, R. L. et al. (2020). Intracellular Cryptococcus neoformans disrupts the transcriptome profile of M1- and M2-polarized host macrophages. *PLoS One* **15**, e0233818. doi:10.1371/journal.pone.0233818
- Subramanian, A., Tamayo, P., Mootha, V. K., Mukherjee, S., Ebert, B. L., Gillette, M. A., Paulovich, A., Pomeroy, S. L., Golub, T. R., Lander, E. S. et al. (2005). Gene set enrichment analysis: a knowledge-based approach for interpreting genome-wide expression profiles. *Proc. Natl. Acad. Sci. USA* **102**, 15545-15550. doi:10.1073/pnas.0506580102
- Testoni, B., Vollenkle, C., Guerrieri, F., Gerbal-Chaloin, S., Blandino, G. and Leverro, M. (2011). Chromatin dynamics of gene activation and repression in response to interferon alpha (IFN $\alpha$ ) reveal new roles for phosphorylated and unphosphorylated forms of the transcription factor STAT2. *J. Biol. Chem.* **286**, 20217-20227. doi:10.1074/jbc.M111.231068
- Trapnell, C., Hendrickson, D. G., Sauvageau, M., Goff, L., Rinn, J. L. and Pachter, L. (2013). Differential analysis of gene regulation at transcript resolution with RNA-seq. *Nat. Biotechnol.* **31**, 46-53. doi:10.1038/nbt.2450
- Varet, H., Brillet-Gueguen, L., Coppee, J. Y. and Dillies, M. A. (2016). SARTools: A DESeq2- and EdgeR-based R pipeline for comprehensive differential analysis of RNA-seq data. *PLoS One* **11**, e0157022. doi:10.1371/journal.pone.0157022
- Waltermann, A., Kartasheva, N. N. and Döbelstein, M. (2003). Differential regulation of p63 and p73 expression. *Oncogene* **22**, 5686-5693. doi:10.1038/sj.onc.1206859
- Wang, N., Liang, H. and Zen, K. (2014). Molecular mechanisms that influence the macrophage m1-m2 polarization balance. *Front. Immunol.* **5**, 614. doi:10.3389/fimmu.2014.00614
- Wilson, H. M. (2014). SOCS proteins in macrophage polarization and function. *Front. Immunol.* **5**, 357. doi:10.3389/fimmu.2014.00357
- Wojciak, J. M., Martinez-Yamout, M. A., Dyson, H. J. and Wright, P. E. (2009). Structural basis for recruitment of CBP/p300 coactivators by STAT1 and STAT2 transactivation domains. *EMBO J.* **28**, 948-958. doi:10.1038/emboj.2009.30
- Wong, L. H., Sim, H., Chatterjee-Kishore, M., Hatzinisiriou, I., Devenish, R. J., Stark, G. and Ralph, S. J. (2002). Isolation and characterization of a human STAT1 gene regulatory element. Inducibility by interferon (IFN) types I and II and role of IFN regulatory factor-1. *J. Biol. Chem.* **277**, 19408-19417. doi:10.1074/jbc.M111302200
- Yahata, T., De Caestecker, M. P., Lechleider, R. J., Andriole, S., Roberts, A. B., Isselbacher, K. J. and Shioda, T. (2000). The MSG1 non-DNA-binding transactivator binds to the p300/CBP coactivators, enhancing their functional link to the Smad transcription factors. *J. Biol. Chem.* **275**, 8825-8834. doi:10.1074/jbc.275.12.8825
- Yahata, T., Takedatsu, H., Dunwoodie, S. L., Braganca, J., Swingler, T., Withington, S. L., Hur, J., Coser, K. R., Isselbacher, K. J., Bhattacharya, S. et al. (2002). Cloning of mouse Cited4, a member of the CITED family p300/CBP-binding transcriptional coactivators: induced expression in mammary epithelial cells. *Genomics* **80**, 601-613. doi:10.1006/geno.2002.7005
- Yan, R., Qureshi, S., Zhong, Z., Wen, Z. and Darnell, J. E. Jr. (1995). The genomic structure of the STAT genes: multiple exons in coincident sites in Stat1 and Stat2. *Nucleic Acids Res.* **23**, 459-463. doi:10.1093/nar/23.3.459
- Yang, D., Guo, J., Divieti, P., Shioda, T. and Bringham, F. R. (2008). CBP/p300-interacting protein CITED1 modulates parathyroid hormone regulation of osteoblastic differentiation. *Endocrinology* **149**, 1728-1735. doi:10.1210/en.2007-0826
- Yoshimura, A., Naka, T. and Kubo, M. (2007). SOCS proteins, cytokine signalling and immune regulation. *Nat. Rev. Immunol.* **7**, 454-465. doi:10.1038/nri2093
- Zafar, A., Pong Ng, H., Diamond-Zaluski, R., Kim, G. D., Ricky Chan, E., Dunwoodie, S. L., Smith, J. D. and Mahabeleshwar, G. H. (2021). CITED2 inhibits STAT1-IRF1 signaling and atherogenesis. *FASEB J.* **35**, e21833. doi:10.1096/fj.20210792R
- Zhang, J. J., Vinkemeier, U., Gu, W., Chakravarti, D., Horvath, C. M. and Darnell, J. E. Jr. (1996). Two contact regions between Stat1 and CBP/p300 in interferon  $\gamma$  signalling. *Proc. Natl. Acad. Sci. USA* **93**, 15092-15096. doi:10.1073/pnas.93.26.15092